Impacts of climate change under CMIP5 RCP scenarios on the streamflow in the Dinder River and ecosystem habitats in Dinder National Park, Sudan

Amir K. Basheer[1, 2], Haishen Lu[1], Abubaker Omer[1], Abubaker B. Ali[3] and Abdeldime M.S. Abdelgader[4, 5]

[1] State Key Laboratory of Hydrology-Water Resources and Hydraulic Engineering, College of Hydrology and Water Resources, Hohai University, Nanjing, 210098, China

[2] Ministry of Agriculture and Irrigation, River Nile State, P.O. Box 8168, Adamer, 12217, Sudan

[3] Research Center of Fluid Machinery & Engineering, National Research Center of Pumps, Key-Lab of Water Saving Irrigation, Jiangsu University, Zhenjiang, China, 212013.

[4] College of Engineering, Karary University, Khartoum, 12304, Sudan

[5] School of information Science and Eng., Southeast University, Nanjing, 210096, China

Correspondence to: Haishen Lu (haishenlu@gmail.com)

Abstract

The fate of seasonal rivers ecosystems habitats under climate change essentially depends on the changes in annual recharge of the river, which related to alterations in precipitation and evaporation over the river basin. Therefore, the change in climate conditions is expected to significantly affect hydrological and ecological components, particularly in fragmented ecosystems. This study aims to assess the impacts of climate change on the streamflow in the Dinder River Basin (DRB), and infer its relative possible effects on the Dinder National Park (DNP) ecosystems habitats in the Sudan. Four global circulation models (GCMs) from Coupled Model Intercomparison Project Phase 5 and two statistical downscaling approaches combined with hydrological model (SWAT) were used to project the climate change conditions over the study periods 2020s, 2050s and 2080s. The results indicated that the climate over the DRB will become warmer and wetter under the most scenarios. The projected precipitation variability

mainly depends on the selected GCM and downscaling approach. Moreover, the projected streamflow is quite sensitive to rainfall and temperature variation, and will likely increase in this century. In contrast to drought periods during (1960s, 1970s and 1980s), the predicted climate change is likely to affect ecosystems in DNP positively and promote the ecological restoration for the habitats of flora and fauna.

1   Introduction

The climate change over the next century expected to severely impact water resources; arid and semi-arid areas are particularly more vulnerable to that change and projected to suffer from water shortage due to precipitation reduction (Tavakoli and De Smedt, 2011;Setegn et al., 2011). Alteration in hydrologic conditions will affect almost every aspect of natural resources and human well-being (Xu, 1999). For instance, ecosystem integrity is influenced either directly or indirectly by climate change and hydrologic variability globally, regionally and at catchment scale. The responses of ecosystems to alterations in the hydrological process usually include complex interactions of biotic and abiotic processes. Hence, the hydrological variability can highly impact the ecosystem species in a variety of ways, such as the linkage between water availability and metabolic and reproductive processes of that species (Burkett et al., 2005). Among all ecosystems, freshwater aquatic ecosystems seem to have the highest proportion of species threatened with extinction caused by climate change (Millennium Ecosystem Assessment, 2005). The empirical framework of (Mantyka-pringle et al., 2012) illustrated that the effects of habitat loss and fragmentation were greatest where maximum temperature of warmest month was highest (i.e., effects were greatest in areas with high temperatures). In contrast, the effects of habitat loss and fragmentation were lowest in areas where precipitation has increased. In other words, smaller effects occurred in areas where average rainfall has increased over time than in areas where rainfall has decreased. This deduced that the maximum temperature and precipitation were the most important variables, with mean temperature change as the third. Thus, both current climate (i.e. maximum temperature) and climate change (i.e. precipitation change) appear to be key determinants of habitat loss and fragmentation effects on terrestrial biodiversity. In some part of the world, ecosystems are already being affected by climate variability. Furthermore, it is very likely that the magnitude and frequency of ecosystem changes will possible rapidly increase and continue in the future (Thomas et al., 2004). As the

2

climate conditions have changed in both precipitation and temperature trends over recent decades, the timing of these events has become vulnerable for alteration as well. According to the Gitay et al. (2002) projections, the ecosystem components in the Northern Hemisphere will experience serious alterations in terms of earlier flowering of plants, migration of birds, animal breeding seasons and emergence of insects. Consequently, under the smallest climatic change scenarios, 18% of species were found to be ''committed to extinction'' while the largest change scenario projected as many as 35% of species to be at risk (Thomas et al., 2004). Many studies investigated the impact of the streamflow change on the freshwater ecosystems, which will probably have strong effects on the system components and abiotic characteristic (Poff and Ward, 1989;Poff and Zimmerman, 2010;Döll and Zhang, 2010;Mantyka-pringle et al., 2012). Erwin (2009), concluded that the wetlands will strongly be influenced due to climate alteration and to overcome all these impacts, assessment of the affect should firstly be conducted. These assessments should be applied, particularly in semi-arid and arid regions which will be more vulnerable areas (Finlayson et al., 2006).

The climate change in the Upper Blue Nile Basin has been addressed by many previous studies using different climate models and techniques (Elshamy et al., 2009;Beyene et al., 2010;Taye et al., 2011;Setegn et al., 2011;Enyew et al., 2014;Gebre et al., 2015). The Dinder River (DR) is one of the largest tributary of the Blue Nile River and major water resource in the Dinder National Park (DNP). It seasonally flows down from western parts of the Ethiopian highlands and flows through the centre of the DNP (AbdelHameed et al., 1997). Seasonality of DR makes it more sensitive to climate change effects, because it mainly depends on seasonal rainfall, which expected to be altered in timing and magnitude. Furthermore, ecosystem habitats in the Dinder river basin (DRB) is basically controlled by the river runoff and climate variables such as temperature and precipitation. Whereas, DNP biodiversity is related to high flow events of DR that influence the river channel shape and allow access to other disconnect floodplain habitats, and to low flow events that limit overall habitats availability and quality. Ecosystem in the DNP contains a group of islands, and wetlands (Mayas) consist of a diverse array of fauna and flora and represent adequate environment for most nutritious grasses to the herbivores, especially during the most severe part of the dry season. Thus, relative changes in hydrological process and climate variables over DRB directly affect the ecosystem habitats and components in the DNP as

general. It should be mentioned that the whole African countries during the last five decades exposed to drought periods, which started in the 1960s and reached the peak in 1984. Consequently, these drought periods affected every African environmental system, particularly Sudan and Ethiopia (Mattsson and Rapp, 1991;Elagib and Elhag, 2011;Masih et al., 2014).

In order to evaluate the effects of climate change on natural resources and maintain ecosystem integrity at the local and territorial scales, further researches should be conducted within the context of water resources management. One of the best tools for simulating current and future prediction of climate change scenarios is GCMs (Xu, 1999). However, there is a general consensus among the scientific community that GCM outputs cannot be used directly as input to hydrological models, which often operate on spatial scales smaller than those of GCMs (Wilby et al., 2002). To predict changes in hydrology and water resources, downscaling the outputs of the GCM on the global scale into the inputs of the hydrological model on the regional scale has been widely applied to obtain the hydrological response (Charlton et al., 2006;Steele-Dunne et al., 2008). Statistical downscaling is thus often used to bridge the scale gap in linking GCM outputs with hydrological models because it does not require significant computing resources and can more directly incorporate observations into method (Fowler et al., 2007). The hydrologic models should provide a link between climate changes and water yields through simulation of hydrologic processes within watersheds. The Soil and Water Assessment Tool (SWAT) is one of the widely used model which has the capability of incorporating the climate change effect for simulation (Ficklin et al., 2010).

Up to the authors' knowledge, the impact of climate change in the DRB has never been thoroughly investigated, and the hydrological alteration affecting the DNP wetland habitats has not been explicitly explored. This paper is the first step toward reporting the impact of climate change on streamflow in the DR and ecosystem habitats in the DNP. The study area has an ecological importance as a national park and biosphere reserve falls on the ecotone between the Sahel and Ethiopian highlands ecoregions. In addition, the change in climate conditions is expected to significantly affect hydrological and ecological components in the DNP fragmented ecosystems. Moreover, projected the hydroclimatic conditions over the DNP and assessed how ecosystem habitats respond to the changes of these variables would provide benchmark information that can be used to increase the capacity of the water resources management and

ecosystem conservation strategies through identify suitable actions for the future. The objectives of this paper are; (1) assess the effect of climate change on the future streamflow magnitude in the DRB, using SWAT model coupled with four GCMs under various climate change scenarios and two downscaling approaches;(2) investigate the potential impact of climate change on the DNP ecosystem components, in order to provide benchmarked information for the decision-makers to be included in adaptation strategies for water resources and environment sustainable development.

The rest of the paper is organized as follows. Section 2 describes the study area and DNP ecosystem components. Section 3 includes a brief description of the SWAT model and two downscaling approaches used to downscale the GCMs model outputs, while the Standardized Precipitation Index (SPI) is also highlighted. Section 4 provides the results and discussion of the projected climate variables and streamflow when applying the two downscaling methods, and investigates the effects of theses variables on the ecosystem habitats. Section 5 concludes this works.

Notations: Table 1 presents a list of all symbols, variables and notations used in this paper.

2   Study area and Dinder national park ecosystem

2.1 Study area

The DR is the largest tributary of the Blue Nile in Sudan. It has a seasonal character where it starts surging in June, peaking around the middle of August each year, and in normal conditions ceases flowing in November. The entire basin ranges in elevation from 2,646 m at an Ethiopian plateau to 407 m at the northwest point where it joined the Blue Nile and its catchment area about 31,422 km^2. DRB geographic coordination is 11°41' to 13°85'N and 34° to 36°20'E (Fig. 1). The average annual discharge for the previous 40 years at the Al Gwisi hydrological station is about 2.2 billion cubic meters (BCM). The main land use and land cover classes in DRB are agriculture, forest, grass, bush, shrubs and others (Abdel Hameed, 1983;Abdel Hameed and Eljack, 2003). Land use of the study area has changed over time due to over increasing population density and agricultural practices. El Moghraby and Abdu (1985), stated that over the past decades there was a remarkable population growth due to the successive migration and

immigration to the Dinder area. Consequently, the related human activities such as farmland expansion for both traditional and mechanized rain-fed agriculture have been dramatically increased. The clay plains of DRB are probably the most striking feature of the geomorphology of Sudan (Whiteman, 1971). There are some types of soil in DRB such as *Eutric Cambisols*, *Chromic Cambisols*, *Eutric Gleysols*, *Eutric Regosols*, *Chromic Vertisols* and *Pellic Vertisols*. The sandy river bed is left with only a few pools which may hold water up to the next rainy season after it ceases to flow (Abdel Hameed, 1983). The annual rainfall amount is normally increased gradually from 500 mm in the north-western part to 1,110 mm in the south-eastern part. The DRB drainage system contains of four sub-drainages namely Khor Galegu drainage system, which is the biggest tributary of the Dinder River, Khor Masaweek, East bank of Dinder River and West bank of Dinder River . Each one of these sub-drainages consists of a number of Mayas, which mainly fed by the main DR stream and its tributaries through distinct feeder channels according to the amount of overflow of the river in flood months (AbdelHameed et al., 1997).

2. 1   Dinder national park ecosystem

The DNP is considered as one of the largest natural reserves in northeast Africa, which was proclaimed as a national park in 1935 following the London Convention (Dasmann, 1972) for the conservation of African flora and fauna. The entire area of DNP is located inside Sudan between longitude 34°30' and 36°00'E and latitude 11°00' and 13°00'N, covering an area of 10,846 km^2 (Fig. 1). The DNP is the only national park north of the 10th parallel, which forms an important ecological zone in the arid and semiarid Sudano-Saharan region. It has high elevation variation ranges from 800 m at an Ethiopian Plateau to about 515 m at the south-eastern part and 100 m at north-eastern part. The Park has unique biodiversity contain a variety with over 250 species of birds, 27 species of large mammals; some of them are listed by the International Union for Conservation of Nature (IUCN) as endangered, vulnerable or threatened species, in addition to an unknown number of smaller mammals. Therefore, the park is considered as adequate habitation for a large number of animals during the dry season and a few numbers when it rains from June through October. The Mammalian fauna leave the Mayas of the park during the rainy season to the high grounds at the east part, in Ethiopia and return with the onset of the dry season. The Mayas are formed by meanders and oxbows along the rivers. It provides

6

dwelling and support for a large number of animal species, such as tiang (*Damaliscus korrigum*), lion (*Panthera leo*), Elephant (*Loxodonta africana*, leopard (*Panthera pardus*), wild dog (*Lycaon pictus*), the red–fronted gazell (*Gazella rufifrons*), greater kudu (*Tragelaphus strepsicerus*), Nubian giraffe (*Giraffa camelopardalis*), black-backed jackal (*Conis mesomelas*), Arabian bustard and greater bustard. There are also numerous hides of insects, which serve a vital function in recycling of the organic compounds (Abdel Hameed and Eljack, 2003).

3 Methods and data

3.1 Hydrological model

Several hydrological models have been developed for application in hydrologic systems and water resources management. One such model utilized in this study is SWAT, which is a distributed watershed-scale hydrological model developed by the United States Department of Agriculture (Arnold et al., 1998). SWAT is a continuous, i.e. a long-term yield model, distributed-parameter hydrological model designed to predict the impact of land management practices on the hydrology and sediment and contaminant transport in agricultural watersheds (Arnold et al., 1998). SWAT subdivides a watershed into sub-basins connected by a stream network, and further delineates hydrologic response units (HRUs) consisting of unique combinations of land cover and soils within each sub-basin. The model assumes that there are no interactions among HRUs, and these HRUs are virtually located within each sub-basin. HRUs delineation minimizes the computational efforts of simulations by lumping similar soil and land use areas into a single unit (Neitsch et al., 2002). SWAT model is broadly documented in many literature (e.g.,Neitsch et al., 2005a;Neitsch et al., 2005b). SWAT provides two methods for estimating surface runoff, which are the SCS curve number and the Green-Ampt infiltration method. The model calculates the peak runoff rate with a modified rational method (Chow et al., 1988). In this study, SWAT was used to simulate streamflow in the DRB. In Arc-SWAT, the basin was divided into 38 subbasins, which were further sub-divided into 116 HRUs based on, soil, land cover and slope attributes. The surface water runoff volume was estimated using the SCS Curve Number method. SWAT was calibrated for the whole basin during the period 1989–1993 based on daily and monthly stream flow at the Al-Gwisi hydrological station and the model inputs. Then, the model further validated over the period 1995 – 1999. The most sensitive

parameters were identified with the built in sensitivity analysis tool in SWAT. We choose 10 most sensitive parameters (Cn2, Alpha_BF, GW_DELAY, Ch_K2, Esco, GWQMN, Ch_N2, GW_REVAP, EPCO, ALPHA_BNK) based on the ranking of sensitivity analysis. Those sensitive parameters were automatically calibrated using the Sequential Uncertainty Fitting (SUFI-2) algorithm (Abbaspour et al., 2007). The Nash–Sutcliffe efficiency coefficient (NS) and the correlation coefficient (R^2) were used to assess the predictive power of the SWAT in this study.

3.2 Global circulation model selection

To investigate the local impact of climate change researchers need to select GCMs able to capture the present-day climate of the study area. Therefore, a comparison between the intra-annual variability of monthly statistics of rainfall (i.e., mean, variance and correlation) and temperature provided by the four GCMs and actual observations is conducted. As the World Meteorological Organization (WMO) recommended the use of the period 1961 – 1990 as a representative period of the present-day climate, since it incorporates some of the natural alterations of the climate, containing both dry (1970s) and wet (1980s) periods (Wigley and Jones, 1987), this period was selected as baseline.

3.3 Statistical downscaling of temperature and rainfall time series

The GCMs outputs resolution is too coarse for regional impact assessment study; therefore, downscaling must be performed before applying GCM outputs into the SWAT model (Dessu and Melesse, 2013). Both change factor (CF) and quantile mapping (QM) downscaling methods were used to downscale GCM outputs.

3.3.1 Change factor downscaling method (CF)

In general, the CF method (Hay et al., 2000;Diaz-Nieto and Wilby, 2005) is an ordinary bias correction method. The CF method is often used to exclude or minimize the bias between observations and the model outputs. The CF procedures rely on modifying the daily time step series of the climate variables such as precipitation and temperature for prediction periods (2020s, 2050s and 2080s) by adding the monthly mean changes of GCM outputs. The adjusted

formulas which are used to modify daily temperature and precipitation are expressed in Eq. (1) and Eq. (2).

$$T_{-adj;\,fur;\,d} = T_{-OBS;\,d} + \sum_{i=1}^{k} pi\left(\overline{T}_{-GCM;\,fur;\,m} - \overline{T}_{-GCM;\,basper;\,m}\right) \tag{1}$$

$$P_{-adj;\,fur;\,d} = P_{-OBS;\,d} \times \sum_{i=1}^{k} pi\left(\overline{P}_{-GCM;\,fur;\,m} / \overline{P}_{-GCM;\,basper;\,m}\right) \tag{2}$$

Where $T_{-adj;\,fur;\,d}$ is the adjusted daily temperature (T_{max} and T_{min}) for the future years, $T_{-OBS;\,d}$ is the observed daily temperature for the baseline years, $T_{-GCM;\,fur;\,m}$ is the monthly mean temperature of the GCM outputs for the future years, $T_{-GCM;\,basper;\,m}$ is the monthly mean temperature of the GCM outputs for the baseline years, pi is the weight of each grid cell and k is the number of the grid cells.

3.3.2 Quantile mapping downscaling method (QM)

The QM is an emerging downscaling approach that utilized to remove bias of observed and simulated rainfall using cumulative distribution functions (CDF). The QM method basically replaces the simulated (GCMs) rainfall/temperature value with the observed value that has the same non-exceedance probability. It shifts the occurrence distributions of precipitation/temperature through creating a transfer function (Sennikovs and Bethers, 2009;Teutschbein and Seibert, 2012). The recommended function for distributions of precipitation events is the Gamma distribution (Thom, 1958) as shown in (Eq. 3).

$$f\gamma(X/\alpha, \beta) = x^{\alpha-1} \cdot \frac{1}{\beta^{\alpha} . \Gamma(\alpha)} \cdot e^{\frac{-x}{\beta}} ; x \geq 0; \alpha, \beta > 0 \tag{3}$$

Where α is shape parameter of Gamma distribution, β is scale parameter of Gamma distribution, f is Distribution function, e is Euler's number, Γ is Gamma function, γ is Gamma distribution, X is Percentile and x is independent (random) variable.

For temperature time series, the Gaussian distribution with location parameter μ and scale parameter σ (Eq. (4)) is usually assumed to fit best (Thom, 1958;Cramér, 1999):

$$fN(X|\mu, \sigma^2) = x^{\alpha-1}.\frac{1}{\sigma.\sqrt{2\pi}}.e^{\frac{-(x-\mu)^2}{2\sigma^2}}; x \in \Re \qquad (4)$$

The scale parameter σ determines the standard deviation, i.e., how much the range of the Gaussian distribution is stretched or compressed. A smaller value for σ results in a more compressed distribution with lower probabilities of extreme values. Contrary, a larger value for σ indicates a stretched shape with higher probabilities of extreme values. The location parameter μ directly controls the mean and, therefore, the location of the distribution.

In this paper, we used an advanced version of QM approach developed recently by Willems et al. (2012). The CDFs were set up on a daily basis for observed (1961 – 1990) and the GCM-simulated rainfall for the baseline period (1961 – 1990). Then the GCM outputs value of a certain day was looked up based on the constructed CDF relative to the GCM simulations with their corresponding cumulative probability (Fig. 2). Subsequently, the same cumulative probability of the precipitation value was located on the empirical CDF of observations. Next, this value was used to adjust the GCM baseline simulation (1961 – 1990). The Gamma CDF (Fγ) and its inverse (Fγ^{-1}) can elucidate this procedure mathematically as follows:

$$P^*_{basper}(d) = F_\gamma^{-1}(F_\gamma(P_{basper}(d)| \alpha_{basper,d}, \beta_{basper,d})| \alpha_{obs,d}, \beta_{obs,d}) \qquad (5)$$

$$P^*_{fut}(d) = F_\gamma^{-1}(F_\gamma(P_{fut}(d)| \alpha_{fut,d}, \beta_{fut,d})| \alpha_{obs,d}, \beta_{obs,d}) \qquad (6)$$

Where P^*_{basper} is precipitation bias corrected for the base period of GCM, P^*_{fut} is precipitation bias corrected for the future period of GCM, F is a cumulative distribution function (CDF), F_γ^{-1} is the inverse of (CDF) and γ is gamma distribution (Willems et al., 2012).

With regard to temperature, the same procedure can be expressed in terms of the Gaussian CDF (FN) and its inverse (F^{-1}N) as:

$$T^*_{basper}(d) = F_N^{-1}(F_N(T_{basper}(d)| \mu_{basper,d}, \sigma^2_{basper,d})| \mu_{obs,d}, \sigma^2_{obs,d}) \qquad (7)$$

$$T^*_{fut}(d) = F_N^{-1}(F_N(T_{fut}(d)| \mu_{fut,d}, \sigma^2_{fut,d})| \mu_{obs,d}, \sigma^2_{obs,d}) \qquad (8)$$

Where T^*_{basper} is temperature bias corrected for the base period of GCM, T^*_{fut} is temperature bias corrected for the future period of GCM, T is temperature, μ is mean (location parameter of Gaussian distribution), σ is standard deviation (scale parameter of Gaussian distribution) and σ^2 is variance (Teutschbein and Seibert, 2012).

The stationarity assumption, i.e., the same correction algorithm applies to both current and future climate conditions, is considered the main drawback of the QM method. Furthermore, the difference between the two downscaling approaches is that the CF method can obtain daily future precipitation time series by adding the average monthly changes of GCM outputs to the observed data. Conversely, QM approach directly adjusted the daily time series generated by the GCM based on linkage of GCM outputs and observed data in the baseline period (Camici et al., 2013).

3. 4   Dryness and wetness pattern over the DRB

Monitoring the drought phenomena and quantifying the wet/dry conditions of the climate are characterized using various drought indices (Kallis, 2008;Mishra and Singh, 2010;Elagib and Elhag, 2011;Elagib, 2013). The Standardized Precipitation Index (McKee et al., 1993) is most widely used to estimate drought indices. SPI quantifies precipitation deficiency at different timescales based on the probability of recording a given quantity of precipitation, and the probabilities are standardized in such way that an index of zero indicates the median precipitation amount. The index is positive for wet conditions, and negative for drought. Although SPI-1, SPI-3, and SPI-6 captured historical drought events, SPI-12 is usually tied to streamflows and reservoir levels at longer timescales. SPI at 12-month is a evaluation of the precipitation for 12 consecutive months compared with that recorded in the same 12 consecutive months in all previous years of available data. Since these timescales are the cumulative results of shorter periods that may be above or below normal conditions, the longer SPIs tend to gravitate toward zero unless a distinctive wet or dry trend is taking place. Moreover, the long-term droughts of 12 months may represent hydrological droughts (Svoboda et al., 2012). Therefore, in this study, SPI at 12-month timescale was computed using observed monthly precipitation at 6 stations from 1961 to 1990 to represents the historical dryness and wetness events over the DRB. For the future, the 90-year SPI-12 series of the rainfall over the DRB was computed for each future precipitation scenario and compared with those from the baseline precipitation. The gamma distribution was chosen in this study for description of the precipitation time series according to McKee et al. (1993) recommendation.

3.5 Data

The topographic data used in this study were generated from a 90 m resolution DEM (digital evaluation model) (Fig. 1) obtained from http://gdex.cr.usgs.gov/gdex/ and processed within Arc-SWAT to provide local elevation, slope, and flow direction. The soil map (1000 m × 1000 m resolution) for the study area was extracted from the digital soil map of the world (FAO) (http://www.fao.org/geonetwork/srv/en/main.home) and African soil map (http://africasoils.net/). Land use map (1 km) in this study was obtained from the land cover institute (LCI) (http://landcover.usgs.gov/). Daily meteorological data, such as temperature and precipitation were collected from Ministry of Water resources and Electricity and other different sources for the period 1961 to 2008. The meteorological data were interpolated using high intensity stations distributed over Blue Nile region. Daily records of the river discharge at the Al-Gwisi hydrological station obtained from the Ministry of Water Resources and Electricity of Sudan were used to calibrate and validate SWAT. Four GCMs have been selected for future climate change projections over the DRB. Table 2 gives an overview of GCMs. The selection of the GCM model was base on other studies related to the impact of climate change on the Upper Blue Nile watershed in Ethiopian plateau. The MPI-ESM-LR and MPI-ESM-MR models as a recent amendment version of ECHAM5 model are recognized to be capable to reproduce the precipitation and temperature pattern in Ethiopian plateau (Beyene et al., 2010;Taye et al., 2011;Enyew et al., 2014;Gebre et al., 2015). The MIROC-ESM and CCSM4 (Jury, 2015) models similarly have been selected (Elshamy et al., 2009;Beyene et al., 2010;Setegn et al., 2011). However, for CCSM4, there is clear difference in rainfall trend (base period) in some months. The RCP4.5 is considered as a moderate mitigation scenario, while RCP8.5 is the higher stabilization pathway, which would provide a wider range of radiative forcing across the RCP extensions. Therefore, RCP4.5 and RCP8.5 might be suitable to study the impact of climate change over DRB and infer the possible response of the DNP ecosystem's habitats, because they have the ability to consider the moderate and extreme scenarios required for planning a better ecosystem restoration management strategy. The daily precipitation, T_{max} and T_{min} from 1961 to 2095 were extracted from grid cells covering the DRB. The period from 1961 – 1990 was defined as the baseline period (denoted by 1980s), while the future periods which covered by this

study are 2006 – 2035, 2036 – 2065 and 2066 – 2095 (denoted by the 2020s, 2050s and 2080s, respectively), except precipitation for CCSM4 model under RCP8.5 scenario (2066 – 2093).

3.6 Climatic condition of the study area

The precipitation and temperature vary spatially and temporally over the DRB. The annual precipitation increases about 30 mm every 10 km from the northwest to the southeast (Ethiopian Plateau), while the temperature decreases with the rainfall increase. Fig. 3 displays the mean monthly rainfall and temperature regimes of all the climate stations in the DRB for the period of 1961–1990. It is clear from Fig. 3 and Table 3 the DRB is hotter in the north-western part, with mean T_{max} of 37.39 °C than the south-eastern part (30.09 °C). The whole basin has a mean T_{max} of 34.77 °C. The hottest months are April and May in the whole basin, while July and August are the coldest ones. The annual rainfall spatial distribution varies conversely with the T_{max}, the Sub-1 (with an annual rainfall of 480.92 mm) and Sub-6 (with an annual rainfall of 1201.12 mm) are the lowest and heaviest stations, respectively.

4   Results and discussions

4.1 Calibration and validation for SWAT model

Firstly, SWAT was calibrated for the whole basin during the period 1989 – 1993 based on daily and monthly stream flow at the Al Gwisi hydrological station and the model inputs. Then, the model further validated over the period 1995–1999. Results showed that SWAT could successfully simulate reasonable daily and monthly streamflow in the DRB as shown in Fig. 4. The coefficient of determination (R^2) and Nash-Sutcliffe coefficient of efficiency values (NSE) were 0.83 and 0.81 for the calibration period and 0.82 and 0.76 during the validation period, respectively. For the daily simulation, R^2 and NSE values were 0.63 and 0.61 for the calibration period and 0.56 and 0.51 for the validation period as listed in Table 4.

4.2 Global circulation models analysis

The annual variability of the monthly mean, variance and autocorrelation of daily precipitation for the four GCM outputs, and the observed data averaged for the period 1961 – 1990 is given in

Fig. 5. For the MPI-ESM-LR and MPI-ESM-MR models, the annual variability of the monthly mean precipitation data is completely well, corresponding to the observed data. For the MIROC-ESM and CCSM4 models, most months were quite well, while other months (April and June) showed clear difference. Furthermore, the MPI-ESM-LR and MPI-ESM-MR models have a general tendency to underestimate the monthly variance throughout the year, while other models have high variance in the some months. For the autocorrelation, the four models have an opposite behavior. Figurer 6 illustrates the comparison between the four GCM outputs, and the observed data for the T_{max} and T_{min} data in terms of monthly mean and variance. The four GCMs are capable to reproduce, the observed mean T_{max} and T_{min} values with small biases. With regard to the variance, the MIROC-ESM and CCSM4 showed clear differences in some months, while the MPI-ESM-LR and MPI-ESM-MR presented slight variance.

In general, the result of the statistical tests on GCMs performance to simulate historical records of climatic variables show better simulation results for temperature than rainfall. The poor result of rainfall simulation is due to GCMs failure to simulate the seasonal migration of the Inter-Tropical Convergence Zone (ITCZ) in these equatorial regions (Wu et al., 2003). It is also attributed to the complex climate system and topography of the Blue Nile basin. For instance, the summer (JJA) rainfall in the catchment is influenced by monsoon activity (Beyene et al., 2010), which might not be accurately considered by the GCMs (Taye et al., 2011).

Taking into account these results and the uncertainties estimated by GCMs, the four models have been selected for representing the actual climate over the DRB. This selection is also supported by the capability of these models to reproduce the mean annual precipitation, which is considered as the main factor leads to huge impact on the DRB and DNP.

4.3 Statistical downscaling of GCMs outputs

Figures 7 and 8 show the results for the downscaling of the annual average T_{max} and T_{min} time series provided by the four models through the CF and QM methods. In the base period comparison between the observed data $(\mathrm{T} - \mathrm{OBS}^{\mathrm{basper}})$ and the results provided by the GCMs before $(\mathrm{T} - \mathrm{GCM}^{\mathrm{basper}})$ and after $(\mathrm{T} - \mathrm{GCM}_{\mathrm{QM}}^{\mathrm{basper}})$, the application of the QM approach is depicted. While, in the future periods (RCP4.5 and RCP8.5) the GCM outputs for future $(\mathrm{T} - \mathrm{GCM}^{\mathrm{fur}})$ and the results provided by the application of the QM $(\mathrm{T} - \mathrm{GCM}_{\mathrm{QM}}^{\mathrm{fut}})$ and CF

methods ($T - OBS_{CF}^{fut}$) are compared. As it is shown in the figures, there is no such big difference between temperature predicted by the MPI-ESM-L, MPI-ESM-MR and MIROC-ESM models when the CF and QM approaches were used, corresponding to their simulated output, whilst the CCSM4 gave remarkable different. Figures 9a displays the relationship between the mean daily T_{max} projected by the two downscaling approaches and GCMs outputs for the study periods. There is slight difference between T_{max} obtained by GCM outputs and that projected by MPI-ESM-LR, MPI-ESM-MR and MIROC-ESM using the two downscaling methods, while under the CCSM4 model, the CF method demonstrated clear difference in the some months. Moreover, the correlation between the mean daily T_{max} projected by the CF, QM and baseline period corresponding to the GCM outputs is illustrated in Fig. 9b. It can be seen that the QM is highly correlated with GCMs outputs in contrast to the CF method. Figure 9c demonstrates the variance of the mean daily T_{max} generated by the CF and QM relative to the simulations of the four GCMs. The MPI-ESM-LR, MPI-ESM-MR and MIROC-ESM models showed slight variance when the CF and QM methods were applied. The CCSM4 model under CF approach showed significant variance in some months compared with the QM method. For the mean daily T_{min} results, it is found that the two downscaling methods obtain the same trend of T_{max} in the mean, correlation and variance values for the four GCMs.

For precipitation, referring to Fig. 10 in the base period, the comparison between the observed data of annual average rainfall time series ($P - OBS^{basper}$) and the results provided by the GCMs before ($P - GCM^{basper}$) and after ($P - GCM_{QM}^{basper}$) the application of the QM approach is depicted. Whereas, the future periods (RCP4.5 and RCP8.5) show the annual average rainfall time series of the GCM outputs before ($P - GCM^{fur}$) and after ($P - GCM_{QM}^{fur}$) applying the QM method and future data obtained by the application of the CF method ($P - OBS_{CF,}^{fut}$). There is a slight difference between the mean annual rainfall projected by the QM approach and GCMs outputs, while the CF elaborates remarkable dissimilarity. For statistical analysis, the relationship between the mean daily rainfall projected by the two downscaling approaches and GCMs outputs for the study periods is shown in Fig. 11a The MPI-ESM-LR and MPI-ESM-MR models showed slight difference in mean daily rainfall when the QM and CF are applied corresponding to their simulated outputs, while the MIROC-ESM and CCSM4 model observed a significant difference when the CF is used. Nevertheless, the MIROC-ESM and CCSM4 model showed insignificant

difference when the QM approach is employed. Figure 11b displays the correlation between the mean daily rainfalls projected using the CF and QM approaches, and the observed data, corresponding to the GCM outputs. The QM method showed high correlation to GCMs outputs compared with the CF method. Figure 11c demonstrates the variance of the mean daily rainfall generated by the CF and QM relative to the simulations of the four GCMs. The QM method showed slight variance when was applied for four models. For the CF approach, the MPI-ESM-LR and MPI-ESM-MR observed slight variance. Conversely, there is a significant variance in mean daily rainfall provided by MIROC-ESM and CCSM4.

4. 4   Historical climate impact

4.4.1   Historical dryness and wetness pattern over the DRB

Figure 12 shows the time series of the SPI on annual bases over the DRB. The SPIs for the 1960s were a mixture of below-and above-normal values, but the first half of the decade had very wet (1.72) and moderately dry (–1.4) conditions in 1963 – 1964 and 1964 – 1965 respectively. The period 1970s saw wet conditions in the first half of the decade with some years lying in the extremely (2.42) in the 1973 – 1974 and moderately wet (1.46) in the 1974 – 1975 while, the latter were near normal records. The 1980s had persistent dry conditions continue until the end of the decade. This period was the driest throughout the study period (moderate and severe dry). The year 1981-1982 was revealed the worst single drought with severe dry condition (1.62). Moreover, the year (1980, 1987) and 1988 were exceptionally near normal to moderate wet respectively.

4.4.2 Impact of climate change during the drought periods (1960s, 1970s and 1980s) on the streamflow and ecosystem

For the best of our knowledge, the DNP ecosystem has three major components namely woodlands (A. Seyal- Balanites), river stream and the Mayas (Wetlands). Moreover, the DNP ecosystem provides sustainable habitations for many species of flora and fauna, which they live or spend in it a part of essential key stages of their annual life cycle. Precisely, river stream and the Mayas which offer sustainable refuge and protection for the living organisms after the flood season, they consider as a valuable store for that reactive link to keep on their flora and fauna

existence until the next flood start and recharge the pools and Mayas (Hakim et al., 1978;Abdel Hameed and Eljack, 2003). The climate change had pronounced effects on the streamflow of DR and the Mayas through changing the precipitation and occurrence of drought waves. The hugely impact of the drought intervals caused significant variability in the water level in the DR and the Mayas during the flood season. These changes could be the main agent in the wetlands ecosystem alteration, and accordingly influenced all the ecosystem components. This consistent with (Woo et al. (1993)) who pointed out that, the fate of the wetlands under climate change is mainly depending to changes in external recharge, which related to alterations in precipitation and evaporation over the wetland itself. Moreover, comparatively tiny increments in precipitation change can significantly influence wetlands flora and fauna at various phases of their lives cycle (Keddy, 2000). As a result, the entire wetland's ecosystem was affected by alterations in precipitation and streamflow (Bauder, 2005). Therefore, according to the seasonality of the DR, small decrease or increase in the annual rainfall leads to decline or increment the water level, and the impact will extend to the next seasons as happened during the drought periods.

The rainfall over the DRB during the first drought period (1963, 1965 and 1969 to 1972) declined about 23 and 11 %, respectively, which led to decline the runoff about 9.8 % during (1972 to 1977). The second wave of drought started in 1976 to 1987 that decreased the rainfall about 14.8 %, led to decrease the runoff about 42.25 % compared to the baseline period (1961 to1971). These alterations caused a sharp decline in the DR runoff and seriously affected the water availability in many Mayas. Moreover, the waves of drought followed by a flood season led to the remarkable damage in the river stream by closing the channels' feeder from the main stream to Mayas and increasing the erosion and sedimentation. Consequently, it decreased the water amounts and many of Mayas dried. There are about 40 Mayas distributed in the DNP such as Ras Amir, Gadahat, and Godah influenced by alterations in the rainfall trend during drought periods. Ras Amir considers as the largest Maya (4.5 km^2), was dried up during the drought periods (1970s) and since that time became less enduring, haphazardly every few years, and full of water in other years. Farash el Naam is the second biggest Maya (1.6 km^2) after drought periods (1980s) became more inconstant and lesser eternal. The last one is Godaha, consists of a series of eleven small Mayas; Godahat is the major one (0.2 km^2), which was affected by the

drought period as well (Hakim et al., 1978;Abdel Hameed, 1983;AbdelHameed et al., 1997;Abdel Hameed and Eljack, 2003). Thus, changes in temperature, precipitation and streamflow magnitude affected the sustainability of ecosystem in terms of the habitats' components in the DNP. Consequently, the damage in habitats impacted most of the flora and fauna in the DNP.

In this century, the DNP habitats virtually certain expose to the climate change impact, such as temperature increment or rainfall increase and/or decline, which will very likely affect the flora and fauna and their migration, blooming and mating timing.

4.5 Future climate change

The CF and QM methods were employed to downscale the climate variables (temperature and precipitation) for the selected GCMs.

4.5.1 Mean of T_{max} and T_{min}

The future climate conditions were determined using the combination of climate change scenarios (RCP 4.5 and RCP 8.5) and four GCM models. Tables 5 and 6 represent the difference between projected T_{max} and T_{min} and the baseline period (1961 – 1990) when the CF and QM methods were applied. T_{max} and T_{min} project a more consistent change trend than precipitation. Stability increases were projected for each variable (T_{max} and T_{min}) by all the models and two emissions scenarios in the futures. The T_{max} trend analysis shows an obvious increment under the two downscaling approaches in the future. For annual mean T_{max} and T_{min}, the MPI-ESM-LR gave the largest increases and MIROC-ESM gave the lowest increases in the future under the two downscaling approaches and scenarios. By using the QM and CF methods, the projected T_{max} increases ranges are between 0.9 °C to 1.8 °C, 1.3 °C to 3.2 °C and 1.6 °C to 5.2 °C in 2020s, 2050s and 2080s respectively. For the annual T_{min} the four models projected increase ranged from 0.9 °C to 1.8 °C, from 1.6 °C to 3.3 °C and from 1.7 °C to 5.3 °C in 2020s, 2050s and 2080s respectively. The RCP8.5 scenario under the QM and CF projected higher temperature increases than the RCP4.5 scenario in the whole periods. Whereas, 2080s period showed the highest increase change in temperature based on the four models. Broadly, the expected temperature under different climate changes scenarios and conditions indicate that the

overall climate will become much warmer as time passes. This result was consistent with the conclusions of (Elshamy et al., 2009;Taye and Willems, 2013;Enyew et al., 2014), which indicated that the temperature projected by multi-GCM will increase over the Upper Blue Nile.

4.5.2 Mean precipitation

Table 7 illustrates the projected change in the annual precipitation under the four GCMs and two scenarios (RCP4.5 and RCP8.5) using the CF and QM downscaling approaches. For annual precipitation, all GCMs projected increase under the two downscaling methods, RCPs and three periods, corresponding to the drought period (1977 – 1988). Mean annual precipitation projected by CCSM4 and MIROC-ESM models generated a dramatic increase when the CF method is applied, while MPI-ESM-LR and MPI-ESM-MR models showed a significant upward trend. The four models under the QM method and two RCPs showed significant and convergent increase during the three periods. The mean annual precipitation changes using the CF method for the four GCMs ranged from 5 to 48.4 %, from 3.2 to 43 % and from 2.6 to 35.4 % under RCP4.5 for the three periods respectively, whereas under RCP8.5 changes ranged from 9 to 50.9 %, from 12.3 to 48.1% and from 9.5 to 44 % in 2020s, 2050s 2080s respectively. Conversely mean annual precipitation projected by using the QM method showed a convergent significant upward trend under the four models. The four models generated increment ranged between 7.8 to 13.1 %, from 7.1 to 14.7 % and from 7.4 to 19.1 % under RCP4.5 for three periods respectively, whereas under RCP8.5 changes ranged from 7.5 to 14.3 %, from 15.7 to 26 % and from 16.8 to 25.3 % in 2020s, 2050s 2080s respectively. Scenario RCP8.5 always suggests a greater increase in precipitation than RCP4.5, especially in 2080s. In general, results showed that the alterations in precipitation amount increases for some months of the year, while it decreases for the other months. Among the future years, the MIROC-ESM, CCSM4 and MPI-ESM-LR under the two downscaling method and RCPs showed the largest value in 2080s. The predicted change magnitudes of the annual precipitation for the four GCMs and the two RCPs using QM methods were consistent during three periods. Broadly, the four GCMs projected upward trends in the annual precipitation in this century. The CCSM4 and MIROC-ESM showed a dramatic increase when the CF method is applied, which may attributed to the difference between the rainfall pattern in the historical period for the GCM model and the study area in some months. In general, studies by (Elshamy et al., 2009;Beyene et al., 2010;Taye et al., 2011;Enyew et al.,

2014) indicated that, the directions of projected precipitation changes are mixed and highly variable both from sub-basin to sub-basin and from season to season over Upper Blue Nile basin.

4.5.3 Response of stream flow to climate change

The highest flow decline which observed to be more influential on the DNP ecosystem habitats was during two drought periods. Accordingly, comparing streamflow in the future periods with that average simulated of the drought periods could produce more reliable results rather than comparing with period including extreme flood years. Therefore, the drought period from 1977 to 1988 which has a low average flow rates (except for 1988) was set as baseline period in this study. The potential effect of future climate change on annual streamflow generated by the outputs of the four models and two downscaling approaches is shown in Table 8 and Fig.13. It can be seen that the expected change rate in 2020s, 2050s and 2080s range from 0.3 to 87.9 %, from 4.7 to 78.1 % and from 2.5 to 87.6 % respectively, for the four models when CF approach is applied. While, the possible annual streamflow changes in the same period, when the QM method applied is predicted to be fluctuated from −11.9 to 9.2 %, from −3.45 to 38.9 % and from −5.7 to 22.4 %. Under the two downscaling methods, RCP8.5 scenario indicated a greater increase in runoff than RCP4.5, particularly in 2080s. The streamflow projected by the MPI-ESM-LR and MPI-ESM-MR under the two downscaling methods showed consistent changes trend with precipitation, particularly when the QM was applied. However, the CCSM4 and MIROC-ESM models under the CF method predicted significant increase trend in the annual streamflow in contrast to the QM method. The CCSM4 and MIROC-ESM models under the QM and RCP4.5 scenario showed decreases in the future periods, except 2080s for the MIROC-ESM which gave a significant increase. Meanwhile, under RCP8.5 the streamflow suggested remarkable increments except the 2020s period for the CCSM4 model which showed significant decline. The increment, which predicted by the CF approach is seemingly due to its high rainfall projection. For the monthly scale, streamflow projected by MPI-ESM-LR and CF method showed reasonable variability in June and October from 4.8 to 2.73 m^3 s^{-1} and from 47.64 to 111 m^3 s^{-1} respectively and changes range of ±46 % in all other months. However, by applying the QM method, streamflow increased significantly in October from 47.64 to 107 m^3 s^{-1}, while other months were fluctuated within ±39 %. The MPI-ESM-MR model through the CF method suggested reasonable variability in streamflow in June and October from 4.8 to 5.1 m^3 s^{-1} and

from 47.64 to 77.1 m^3 s^{-1} respectively, and alterations range of ±84 % in all other months. While, by applying the QM method, streamflow increased significantly in October from 47.64 to 140 m^3 s^{-1}, while other months were fluctuated within ±95 %. The mean monthly streamflow projected by the CF method in 2020s under the CCSM4 and MIROC-ESM model showed remarkable increases in June and October from 4.8 to 7.9 m^3 s^{-1} and from 47.64 to 165.1 m^3 s^{-1} respectively, and varied with percentage rate of 87 % in the other months. While, by applying the QM method to the same models, monthly streamflow in June and October observed to increase from 4.8 to 5.4 and from 47.64 to 160 m^3 s^{-1} respectively, and fluctuated within ±93 % in the other months. Although the percentage of streamflow increment in 2050 was somewhat less than that of 2020s, the prediction of the four GCMs and the two approaches generally showed a similar upward trend in the two periods. Similar to 2020s and 2050s, the monthly streamflow predictions for future period 2080s showed the upward trend with a slight difference in the magnitude in some months comparing to baseline period. The high percentage of change in monthly streamflow which displayed by CCSM4 and MIROC-ESM models under the CF and QM approaches could be attributed to the uncertainty of the models and the difference in the pattern of some monthly rainfall between the model and the study area. Furthermore, the DR is a seasonal river (June - October) flows from elevation 2646 m to 400 m thus, runoff is rapid and a small amount of precipitation is retained by deep percolation (UNESCO, 2004). Moreover, as mountain region, the streamflow in the DR showed high sensitivity to precipitation changes particularly in the last five decades. Although the CCSM4 and MIROC-ESM models under the QM method and RCP4.5 showed an increment in rainfall projection in the three periods, the streamflow projected decrease. This could be owing to the uncertainty of hydrological model parameters. Among the four models, MPI-EMI-LR and MPI-ESM-MR projected reasonable increment in streamflow over the study area.

Despite the projected streamflow varied between increase and decline, the increase trend was the dominate characteristic in streamflow prediction. Based on the results obtained in this study, there is an uncertainty in the simulated streamflow under given climate change conditions, this uncertainty can be attributed to different sources of variability represented in future emissions scenarios, GCMs projections, downscaling approaches and hydrological model parameterization.

4.5.4 Future dryness and wetness pattern over the DRB

The future rainfall time series projected by the four GCMs and the two downscaling approaches were analyzed by applying the SPI-12 to investigate the hydrological wetness/dryness events (Fig. 14 and 15). In general, the future dryness/wetness of the DRB showed a different trend than the past. Results showed that compared to the baseline period, severity dry and very wet conditions are expected to increase, but the duration is expected to decrease. In the other words, dry/wet conditions will likely become more frequent during the next ten decades, i.e. it recurs at shorter time intervals, in particular when the QM approach is applied. However, for the future projected using the CF methods, the dryness/wetness suggested a symmetric pattern to the baseline period (Fig. 15). For the MPI-ESM-LR model under the QM method and the two RCP scenarios, the annual dryness/wetness events during three periods projected to be range from 10 to 23 % dry (moderately-sever-extreme) and from 10 to 24 % wet (moderately-very-extreme) while the remaining are near moderate. Moreover, dry/wet conditions are likely became less frequent, but it presumably be increased in term of severity, particularly in 2050s. For the MPI-ESM-MR model under the QM method, the percentage of dry years suggested to be range between 7 to 23 %, while the wet ones (moderately-very-extreme) ranged between 13 to 23 %. The RCP4.5 scenario in 2050s and 2080s gave extreme dry and wet events, while RCP8.5 scenario predicted the same events in 2050s. The dry conditions that projected by MIROC-ESM model using QM method, were found to be range from 6 to 20 % (moderately-very-extreme), whilst wet conditions ranged between 10 to 23 % (moderately-very-extreme) during the three periods. Under RCP8.5 and the QM method, the 2050s and 2080s suggested having long duration of severe and moderate draught. Regarding to the CCSM4 model under RCP8.5 scenario and the QM method, in 2020s projected to have moderate-sever dry conditions (27 %) whereas, the wetness condition was found to be 7 %. Conversely, 2080s showed highest percentage of wetness events (30 %) while the dryness events were 16%.

4.5.5   Impact of projected climate change on DNP ecosystem habitats

Based on the climate change projections scenarios, the changes in temperature and precipitation will impact either directly or indirectly the streamflow magnitude. Consequently, the DNP ecosystem will very likely be exposed to a variety of negative and positive effects based on these

22

projections. Although climatic warming in this century is expected to start a drying trend in wetland ecosystems in most parts of the world (Gorham, 1991), the results obtained by this work accomplished that the DRB wetlands will experience increment in water magnitude according to the projected increment in the annual rainfall and streamflow. Generally, the temperature increase and greater changes in precipitation will occur in the DNP over this century. The Four GCMs projected annually increases in T_{max} ranged from 0.9 to 4.9 ℃ and T_{min} ranged from 0.9 to 5.3 ℃, whilst the RCP8.5 scenario projected the greatest increase. Alterations in precipitation are projected to temporally vary when the CF and QM approaches applied between 2.6 to 50.6 % and between 7.1 to 26 % respectively. The DNP is expected to get drier in the summer, whereas more likely to be wetter in autumn. The rainfall increment will be greater in the southeast part of DNP more than the northwest. Moreover, the maximum magnitude of precipitation, will likely increase as well.

The upward trend in the rainfall amount which predicted by the four models will have distinctive positive impacts on the DNP ecosystems in terms of habitats sustainability of many living organisms. The four GCM models when the CF and QM approaches applied, projected increase in rainfall over the DRB ranged between 2.6 to 50.6 % and between 7.1 to 26 % respectively, which will likely lead to an increment in streamflow. Furthermore, the long duration of hydrological dryness that happened in the past which led to the huge impact in the DNP ecosystem, was projected to decrease. These increases in the streamflow likely will be suitable amounts to restoration of the DNP ecosystem components. The DNP lies on the road of winter migration for many African birds during their pass to eastern Africa Rift valley lakes or southward. Accordingly, the increase of water during the flood season in this century will lead to increase the capacity of the Mayas and pools to receive more numbers of these migrant birds. Furthermore, these habitats will not be a breed effective threat and danger on the life cycle for that birds and defect on the ecosystem balance of DNP and regional scale. Otherwise, the four GCMs predictions indicated that precipitation most probably tends to increase in the future over the DNP. Consequently, this positive variation will likely greatly influence the water level in the Mayas and pools and promote the intensity of vegetation cover and growing of the grasses which are considered as a major food source for most the DNP fauna.

The analysis presented here indicates that the four GCMs and the two scenarios projected significant annually and monthly increment in temperature. This increment will likely affect the habitats' component in the DNP, as the water level will be affected by the evapotranspiration over the DRB, particularly under the MPI-ESM-LR and MPI-ESM-MR models and RCP8.5 scenario at the end of this century.

According to the projected alterations in the temperature, precipitation and streamflow, we expected that the DNP ecosystems events, and habitats will very likely to be shifted. In fact, the spatial and temporal of the temperature and precipitation over the DNP offer DNP ecosystem the same habitat with different climatic conditions. Consequently, most of the fauna and flora have high resilience to adapt to the impact of the climate change and habitats loss as happened during drought periods. This implies that, during drought periods some of the fauna and flora have changed their habitats to the areas that have the same climate conditions of their previous habitats as a form of adaptation. Furthermore, over the last 100 years, maximum temperature with mean rainfall as secondary driver was the determinant factor in habitat loss and fragmentation, averaged across species and geographic regions. Habitat loss and fragmentation effects were greatest in areas with high maximum temperatures. Conversely, they were lowest in areas where average rainfall has increased over time (Mantyka-pringle et al., 2012). Based on the projected climate determinants and the DNP ecosystem characteristics, it can be concluded that, ecosystem components will likely expect to start restoration of ecosystem habitats.

5 Conclusion

This paper analyzed the response of streamflow and ecosystem habitats in the DRB to possible future climate conditions change that predicted by using four GCMs coupled with two downscaling approaches and physically based distributed hydrologic model (SWAT). Moreover, the future rainfall time series projected by the four GCMs were analyzed by applying the SPI-12 to estimate the hydrological dryness/wetness events over the DRB during three periods. Predictions of the four GCMs pointed out the temperature and precipitation will increase in the next century, while the severe dry and very wet events of short durations are predicted to be more frequent in the future. Consequently, the streamflow is likely to increase according to the rainfall increase. Type of the used downscaling approach was the key factor in climatic variables' projection. The annual rainfall predicted by using the QM approach based on the four

GCM models tend to have the same increasing trend, particularly under RCP8.5 scenario. The CF approach showed huge increment with the CCSM4 and MIROC-ESM models corresponding to the other models. In contrast, the MPI-ESM-LR and MPI-ESM-MR models under the CF and QM approaches, predicted convergent annual rainfall upward trend. The similarity of the result obtained by applying the QM method for the four GCM models was regarded to the fact that the QM approach takes into account daily rainfall time series generated by the GCM. There is uncertainty in the Streamflow projection basically depend on the GCMs, scenarios, downscaling approach and model parameterization. Relying on prediction of potential possible changes in climate condition, ecosystem components in the DNP substantially will likely be affected in a way that make that living organism habitats and life cycle have recovery conditions rather than extinction and destruction circumstances, as it was happening during the drought periods (1960s, 1970s and 1980s). On the other hand, the projected rainfall and the seasonality of the river will make more uneven distribution of annual flow from year to another. Thus, high attentions to extreme events (floods and drought) to avoid the negative hydrological effect on the DNP ecosystem habitats should be considered. This study projected the hydroclimatic condition over the DNP and assessed how ecosystem habitats respond to the changes of these variables. Although the presences of the uncertainties, the results provide benchmark information that can be used to increase the capacity of the water resources management and ecosystem conservation strategies through identify suitable actions for the future. That is to create more resilience to climate changes related to habitats restoration and continued management of other stressors in the DNP ecosystem. Furthermore, integrity of hydrological conditions in the DR stream and Mayas' should be considered, to reduce the negative impact of climate change on fragmented wetlands' ecosystem, particularly in terms of dryness and wetness events. Finally, this work would offer quite useful information required by rain-fed agriculture, hydrologists, ecologists and zoologist for further researches.

ACKNOWLEDGMENTS

References

Abbaspour, K. C., Yang, J., Maximov, I., Siber, R., Bogner, K., Mieleitner, J., Zobrist, J., and Srinivasan, R.: Modelling hydrology and water quality in the pre-alpine/alpine Thur watershed using SWAT, Journal of hydrology, 333, 413-430, 2007.

Abdel Hameed, S. M.: Vegetation of the mayas of Dinder National Park, Sudan, Colorado State University, 1983.

Abdel Hameed, S. M., and Eljack, A. O.: Ramsar Information Sheet (RIS) for Dinder national park, Sudan, Wetlands International Global. Available athttps://rsis.ramsar.org/RISapp/files/RISrep/SD1461RIS.pdf (accessed April 1, 2015). 2003.

AbdelHameed, S. M., Awad, N. M., ElMoghraby, A. I., Hamid, A. A., Hamid, S. H., and Osman, O. A.: Watershed management in the Dinder National Park, Sudan, Agricultural and forest meteorology, 84, 89-96, 1997.

Arnold, J. G., Srinivasan, R., Muttiah, R. S., and Williams, J. R.: Large area hydrologic modeling and assessment part I: Model development1, in, Wiley Online Library, 1998.

Bauder, E.: The effects of an unpredictable precipitation regime on vernal pool hydrology, Freshwater Biology, 50, 2129-2135, 2005.

Beyene, T., Lettenmaier, D. P., and Kabat, P.: Hydrologic impacts of climate change on the Nile River Basin: implications of the 2007 IPCC scenarios, Climatic change, 100, 433-461, 2010.

Burkett, V. R., Wilcox, D. A., Stottlemyer, R., Barrow, W., Fagre, D., Baron, J., Price, J., Nielsen, J. L., Allen, C. D., and Peterson, D. L.: Nonlinear dynamics in ecosystem response to climatic change: case studies and policy implications, Ecological complexity, 2, 357-394, 2005.

Camici, S., Brocca, L., Melone, F., and Moramarco, T.: Impact of climate change on flood frequency using different climate models and downscaling approaches, Journal of Hydrologic Engineering, 19, 04014002, 2013.

Charlton, R., Fealy, R., Moore, S., Sweeney, J., and Murphy, C.: Assessing the impact of climate change on water supply and flood hazard in Ireland using statistical downscaling and hydrological modelling techniques, Climatic change, 74, 475-491, 2006.

Chow, V. T., Maidment, D. R., and Mays, L. W.: Applied hydrology, 1988.

Cramér, H.: Mathematical methods of statistics, Princeton university press, 1999.

Dasmann, W.: Development and management of Dinder National Park and its Wildlife, Food and Agriculture Organisation, Rep, 3113, 2-62, 1972.

Dessu, S. B., and Melesse, A. M.: Impact and uncertainties of climate change on the hydrology of the Mara River basin, Kenya/Tanzania, Hydrological Processes, 27, 2973-2986, 2013.

Diaz-Nieto, J., and Wilby, R. L.: A comparison of statistical downscaling and climate change factor methods: impacts on low flows in the River Thames, United Kingdom, Climatic Change, 69, 245-268, 2005.

Döll, P., and Zhang, J.: Impact of climate change on freshwater ecosystems: a global-scale analysis of ecologically relevant river flow alterations, Hydrology and Earth System Sciences, 14, 783-799, 2010.

El Moghraby, A., and Abdu, A.: The Dinder National Park, study area. Final report, Environmental management in the Sudan. Institute of Environmental Studies, University of Khartoum Reports, 45, 1985.

Elagib, N. A., and Elhag, M. M.: Major climate indicators of ongoing drought in Sudan, Journal of Hydrology, 409, 612-625, 2011.

Elagib, N. A.: Meteorological drought and crop yield in sub-Saharan Sudan I, J. Water Resour. Arid Environ., 3, 164-171, 2013.

Elshamy, M. E., Seierstad, I. A., and Sorteberg, A.: Impacts of climate change on Blue Nile flows using bias-corrected GCM scenarios, Hydrology and Earth System Sciences, 13, 551-565, 2009.

Enyew, B., Van Lanen, H., and Van Loon, A.: Assessment of the Impact of Climate Change on Hydrological Drought in Lake Tana Catchment, Blue Nile Basin, Ethiopia, J Geol Geosci, 3, 2, 2014.

Erwin, K. L.: Wetlands and global climate change: the role of wetland restoration in a changing world, Wetlands Ecology and management, 17, 71-84, 2009.

Ficklin, D. L., Luo, Y., Luedeling, E., Gatzke, S. E., and Zhang, M.: Sensitivity of agricultural runoff loads to rising levels of CO 2 and climate change in the San Joaquin Valley watershed of California, Environmental Pollution, 158, 223-234, 2010.

Finlayson, C., Gitay, H., Bellio, M., van Dam, R., and Taylor, I.: Climate variability and change and other pressures on wetlands and waterbirds: impacts and adaptation, Waterbirds around the world, 88-97, 2006.

Fowler, H., Blenkinsop, S., and Tebaldi, C.: Linking climate change modelling to impacts studies: recent advances in downscaling techniques for hydrological modelling, International journal of climatology, 27, 1547-1578, 2007.

Gebre, S., Tadele, K., and Mariam, B.: Potential Impacts of Climate Change on the Hydrology and Water resources Availability of Didessa Catchment, Blue Nile River Basin, Ethiopia, J Geol Geosci, 4, 2, 2015.

Gitay, H., Suárez, A., Watson, R. T., and Dokken, D. J.: Climate change and biodiversity, Intergovernmental Panel on Climate Change, Geneva, 2002.

Gorham, E.: Northern peatlands: role in the carbon cycle and probable responses to climatic warming, Ecological applications, 1, 182-195, 1991.

Hakim, S., Fadlalla, B., Awad, N. M., and Wahab., S. A.: Ecosystems of the vegetation of Dinder national park. Unpublished report. Wildlife Research Unit, Khartoum, Sudan. , 1978.

Hay, L. E., Wilby, R. L., and Leavesley, G. H.: A comparison of delta change and downscaled GCM scenarios for three mounfainous basins in THE UNITED STATES1, JAWRA Journal of the American Water Resources Association, 36, 387-397, 2000.

Jury, M. R.: Statistical evaluation of CMIP5 climate change model simulations for the Ethiopian highlands, International Journal of Climatology, 35, 37-44, 2015.

Kallis, G.: Droughts, Annual Review of Environment and Resources, 33, 85, 2008.

Keddy, P.: Wetland Ecology: Principles and Conservation. 2000, Cambridge, UK: Cambridge University Press, 2000.

Mantyka-pringle, C. S., Martin, T. G., and Rhodes, J. R.: Interactions between climate and habitat loss effects on biodiversity: a systematic review and meta-analysis, Global Change Biology, 18, 1239-1252, 2012.

Masih, I., Maskey, S., Mussá, F., and Trambauer, P.: A review of droughts on the African continent: a geospatial and long-term perspective, Hydrology and Earth System Sciences, 18, 3635-3649, 2014.

Mattsson, J. O., and Rapp, A.: The recent droughts in western Ethiopia and Sudan in a climatic context, Ambio, 172-175, 1991.

McKee, T. B., Doesken, N. J., and Kleist, J.: The relationship of drought frequency and duration to time scales, Proceedings of the 8th Conference on Applied Climatology, 1993, 179-183,

Millennium Ecosystem Assessment: Ecosystems and human well-being: biodiversity synthesis, Island Press Washington, DC, 2005.

Mishra, A. K., and Singh, V. P.: A review of drought concepts, Journal of Hydrology, 391, 202-216, 2010.

Neitsch, S., Arnold, J., Kiniry, J., Srinivasan, R., and Williams, J.: Soil and Water Assessment Tool User's Manual: Version 2000. GSWRL Report 02-02, BRC Report 02-06, Publ. Texas Water Resources Institute, TR-192, College Station, Texas, 2002.

Neitsch, S., Arnold, J., Kiniry, J., Srinivasan, R., and Williams, J.: Soil and water assessment tool input/output file documentation, Blackland Research Center, Temple, Texas, 2005a.

Neitsch, S., Arnold, J., Kiniry, J., Williams, J., and King, K.: Soil and water assessment tool theoretical documentation. Grassland, Soil and Water Research Laboratory, Temple, TX, 2005b.

Poff, N. L., and Ward, J. V.: Implications of streamflow variability and predictability for lotic community structure: a regional analysis of streamflow patterns, Canadian journal of fisheries and aquatic sciences, 46, 1805-1818, 1989.

Poff, N. L., and Zimmerman, J. K.: Ecological responses to altered flow regimes: a literature review to inform the science and management of environmental flows, Freshwater Biology, 55, 194-205, 2010.

Sennikovs, J., and Bethers, U.: Statistical downscaling method of regional climate model results for hydrological modelling, Proc. 18 th World IMACS/MODSIM Congress, Cairns, Australia, 2009,

Setegn, S. G., Rayner, D., Melesse, A. M., Dargahi, B., and Srinivasan, R.: Impact of climate change on the hydroclimatology of Lake Tana Basin, Ethiopia, Water Resources Research, 47, 2011.

Steele-Dunne, S., Lynch, P., McGrath, R., Semmler, T., Wang, S., Hanafin, J., and Nolan, P.: The impacts of climate change on hydrology in Ireland, Journal of Hydrology, 356, 28-45, 2008.

Svoboda, M., Hayes, M., and Wood, D.: Standardized precipitation index user guide, World Meteorological Organization Geneva, Switzerland, 2012.

Tavakoli, M., and De Smedt, F.: Impact of climate change on streamflow and soil moisture in the Vermilion Basin, Illinois, Journal of Hydrologic Engineering, 2011.

Taye, M. T., Ntegeka, V., Ogiramoi, N., and Willems, P.: Assessment of climate change impact on hydrological extremes in two source regions of the Nile River Basin, Hydrology and Earth System Sciences, 15, 209-222, 2011.

Taye, M. T., and Willems, P.: Influence of downscaling methods in projecting climate change impact on hydrological extremes of upper Blue Nile basin, Hydrology and Earth System Sciences Discussions, 10, 7857-7896, 2013.

Teutschbein, C., and Seibert, J.: Bias correction of regional climate model simulations for hydrological climate-change impact studies: Review and evaluation of different methods, Journal of Hydrology, 456, 12-29, 2012.

Thom, H. C.: A note on the gamma distribution, Monthly Weather Review, 86, 117-122, 1958.

Thomas, C. D., Cameron, A., Green, R. E., Bakkenes, M., Beaumont, L. J., Collingham, Y. C., Erasmus, B. F., De Siqueira, M. F., Grainger, A., and Hannah, L.: Extinction risk from climate change, Nature, 427, 145-148, 2004.

UNESCO: Water Development Report for Ethiopia, Water Development Report for Ethiopia. UN-WATER/ WWAP/2006/7, World Water Assessment Program Report, MOWR, Addis Ababa, Ethiopia.\, 2004.

Whiteman, A.: Tho Geology of the Sudan Republic, 1971.

Wigley, T., and Jones, P.: England and Wales precipitation: a discussion of recent changes in variability and an update to 1985, Journal of Climatology, 7, 1-246, 1987.

Wilby, R. L., Dawson, C. W., and Barrow, E. M.: SDSM—a decision support tool for the assessment of regional climate change impacts, Environmental Modelling & Software, 17, 145-157, 2002.

Willems, P., Olsson, J., Arnbjerg-Nielsen, K., Beecham, S., Pathirana, A., Gregersen, I. B., Madsen, H., and Nguyen, V.: Impacts of Climate Change on Rainfall Extremes and Urban Drainage Systems, IWA Publishing Company, 2012.

Woo, M.-K., Rowsell, R. D., and Clark, R. G.: Hydrological classification of Canadian prairie wetlands and prediction of wetland inundation in response to climatic variability, 79, Canadian Wildlife Service Saskatoon, Canada, 1993.

Wu, X., Liang, X. Z., and Zhang, G. J.: Seasonal migration of ITCZ precipitation across the equator: Why can't GCMs simulate it?, Geophysical research letters, 30, 2003.

Xu, C.-y.: Climate change and hydrologic models: A review of existing gaps and recent research developments, Water Resources Management, 13, 369-382, 1999.

Table 1. Symbols, variables and notations

Symbols	
a, b	Parameter
adj	adjusted
α	Shape parameter of Gamma distribution
β	Scale parameter of Gamma distribution
$basper$	Baseline period (1961-1990)
CDF	Cumulative distribution function
CF	Change factor method
d	daily
e	Euler's number
f	Distribution function
F	Cumulative distribution function (CDF)
F^{-1}	Inverse of CDF
fur	Future period (2020s, 2050s and 2080s)
Γ	Gamma function
k	number of the grid cells
m	month
N	Gaussian (normal) distribution
μ	Mean (location parameter of Gaussian distribution)
OBS	Observed data (day)
P	Precipitation (mm)
pi	the weight of each grid cell
σ	Standard deviation (scale parameter of Gaussian distribution)
σ^2	Variance
T	Temperature (°C)
x	Independent (random) variable
X	Percentile
γ	Gamma distribution
$*$	final bias-corrected

Table 2. Information of the climate models.

Model name	Model centre	Grid resolution
CCSM4	the National Centre for Atmospheric Research, USA	0.9424° x 1.25°
MIROC-ESM	JAMSTEC, AORI, and NIES, Japan	2.7906° x 2.8125°
MPI-ESM-LR	Max-Planck-Institute for Meteorology, Hamburg, Germany	1.8653° x 1.875°
MPI-ESM-MR	Max-Planck-Institute for Meteorology, Hamburg, Germany	1.865° x 1.875°

Table 3. Statistics of climate stations for the period of 1961-1990 in the DRB.

Sub-station	Elevation	Annual rainfall (mm)	Mean Tmax (ºC)	Mean Tmin (ºC)
Sub-1	425	480.92	37.39	21.49
Sub-2	442	630.16	36.81	21.53
Sub-3	487	716.34	36.23	18.84
Sub-4	714	894.04	32.09	21.19
Sub-5	824	1042.6	33.49	17.73
Sub-6	886	1201.12	30.09	16.15

Table 4. Calibration (1989–1993) and validation (1995–1999) for the SWAT model.

Period	Monthly		Daily	
	NS	R^2	NS	R^2
Calibration (1989-1993)	0.81	0.83	0.62	0.63
Validation (1995-1999)	0.76	0.82	0.51	0.56

Table 5. Annual changes in T_{max} in the future under the four GCMs and two scenarios (RCP4.5 and RCP8.5).

Period's	Annual change in T$_{max}$ (ºC)							
	CF method				QM method			
RCP 4.5	MPI-ESM-LR	MPI-ESM-MR	MIROC-ESM	CCSM4	MPI-ESM-LR	MPI-ESM-MR	MIROC-ESM	CCSM4
2020s	1.4	1.2	0.9	0.9	1.7	1.2	0.7	0.8
2050s	2.4	2.4	1.5	1.5	2.7	2.4	1.3	1.5
2080s	3.0	2.9	1.9	1.7	3.2	2.9	1.6	1.7
RCP 8.5								
2020s	1.6	1.4	0.6	1.0	1.8	1.5	0.6	1.2
2050s	2.9	2.9	1.4	1.9	3.2	3.0	1.3	2.1
2080s	4.9	4.8	3.3	3.5	5.2	4.7	3.3	3.7

Table 6. Annual changes in T_{min} in the future under the four GCMs and two scenarios (RCP4.5 and RCP8.5).

Period's	Annual change in T$_{min}$ (ºC)							
	CF method				QM method			
RCP 4.5	MPI-ESM-LR	MPI-ESM-MR	MIROC-ESM	CCSM4	MPI-ESM-LR	MPI-ESM-MR	MIROC-ESM	CCSM4
2020s	1.4	1.4	1.2	0.9	1.6	1.3	1.2	1.0
2050s	2.4	2.6	2.0	1.6	2.6	2.4	1.9	1.9
2080s	2.9	3.1	2.5	1.7	3.1	2.9	2.5	2.1
RCP 8.5								
2020s	1.6	1.7	1.0	1.0	1.8	1.5	1.0	1.5
2050s	3.0	3.3	2.1	1.9	3.2	2.9	2.2	2.7
2080s	5.1	5.3	4.3	3.4	5.3	4.9	4.3	4.4

Table 7. Annual changes in precipitation in the future under RCP4.5 and RCP8.5 scenarios for the GCMs.

Period's	Annual change in precipitation (%)							
	CF method				QM method			
RCP 4.5	MPI-ESM-LR	MPI-ESM-MR	MIROC-ESM	CCSM4	MPI-ESM-LR	MPI-ESM-MR	MIROC-ESM	CCSM4
2020s	8.1	5	11	48.4	13.1	10.3	7.8	12
2050s	7.2	3.2	18.4	43	13.6	7.1	12.9	14.7
2080s	8.9	2.6	29.9	35.4	14.8	7.4	19.1	17
RCP 8.5								
2020s	10.8	9	24.2	50.6	14	7.5	11.1	14.3
2050s	15.4	12.3	48.1	47.7	17.2	15.7	26	20.7
2080s	16.7	9.5	38.2	44	25.3	16.8	22	21.7

Table 8. Possible annual streamflow changes in the future years (2020s, 2050s and 2080s) of the DRB.

Period's	Annual change in streamflow (%)							
	CF method				QM method			
RCP 4.5	MPI-ESM-LR	MPI-ESM-MR	MIROC-ESM	CCSM4	MPI-ESM-LR	MPI-ESM-MR	MIROC-ESM	CCSM4
2020s	23.5	15.3	29.5	87.9	9.2	-2.1	-9.4	-8.5
2050s	19.9	4.7	55.0	78.1	5.1	-3.45	-2.1	-0.41
2080s	26.5	2.5	66.4	82.8	11.4	4.2	12.3	-5.7
RCP 8.5								
2020s	27.3	0.3	61.3	86.7	3.1	-7.1	13.4	-11.9
2050s	37.1	23.2	78.2	71.0	5.9	10.8	38.9	3.1
2080s	44.3	17.0	81.3	87.6	22.4	6.9	15.7	9.0
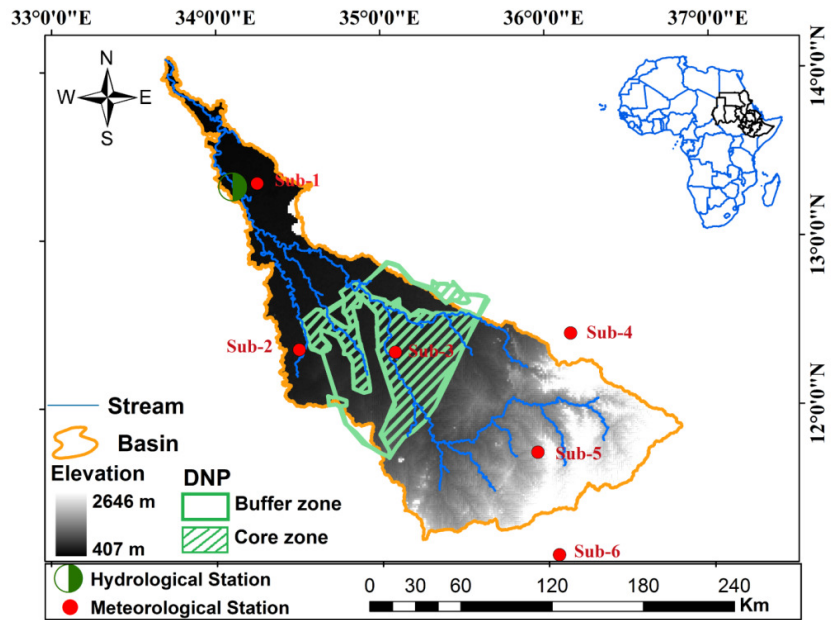
Figure 1. Topography (m) of the DRB based on a 90 m DEM and geographic locations of DNP and hydrological and meteorological stations.
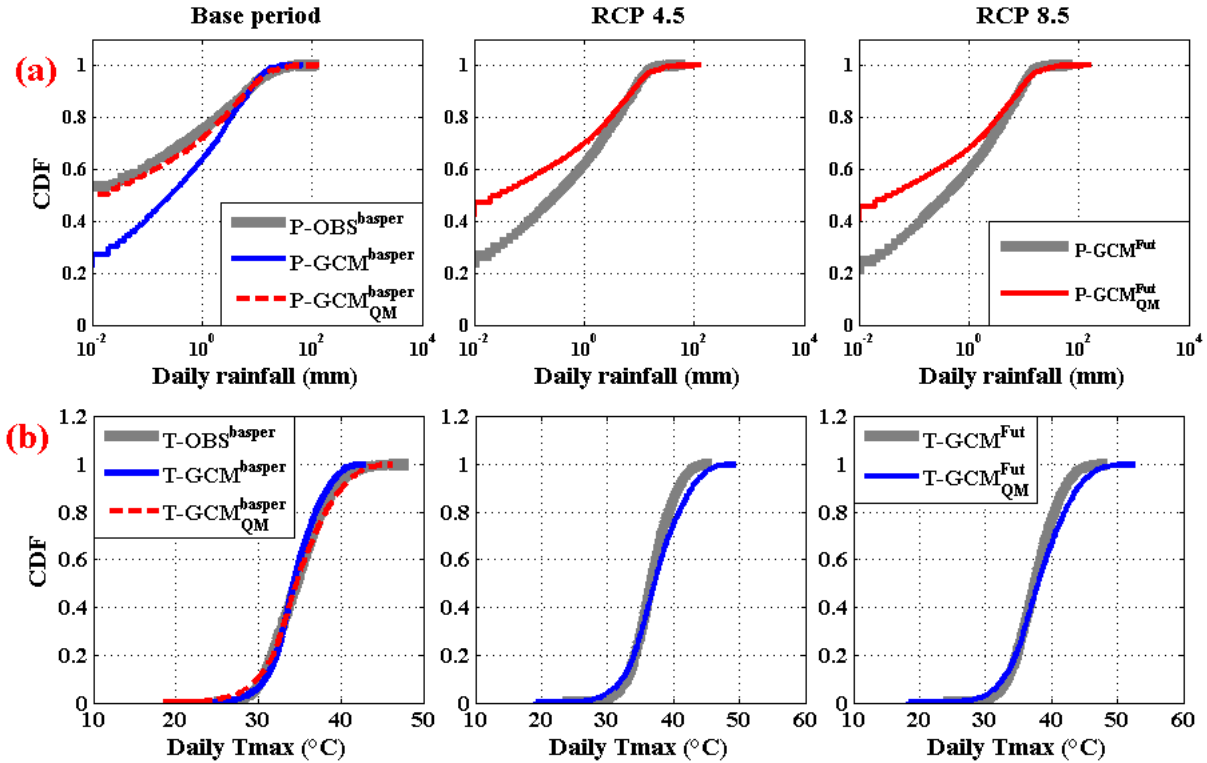
Figure 2. (a) Comparison between the empirical cumulative density function of the observed rainfall data and the one provided by the MIROC-ESM model, before (dashed line) and after (solid line) the application of the QM method: the Based period; and future climate (RCP4.5 and RCP8.5); over the study area. (b) Same comparison done for T_{max} by using Gaussian distribution for the MPI-ESM-LR model.
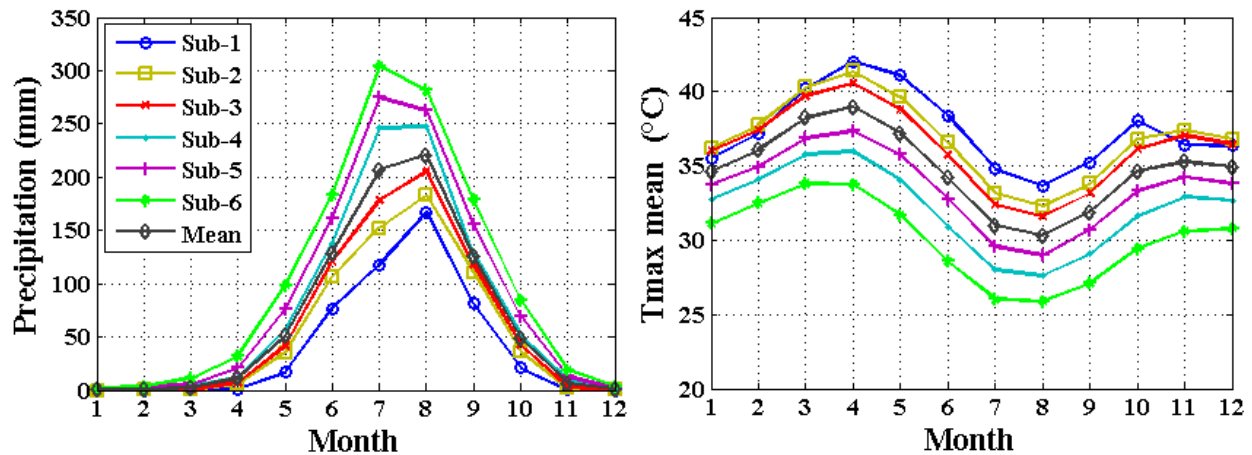
Figure 3.The mean monthly rainfall and T_{max} regimes of all the climate stations used in this study for the period of 1961–1990.
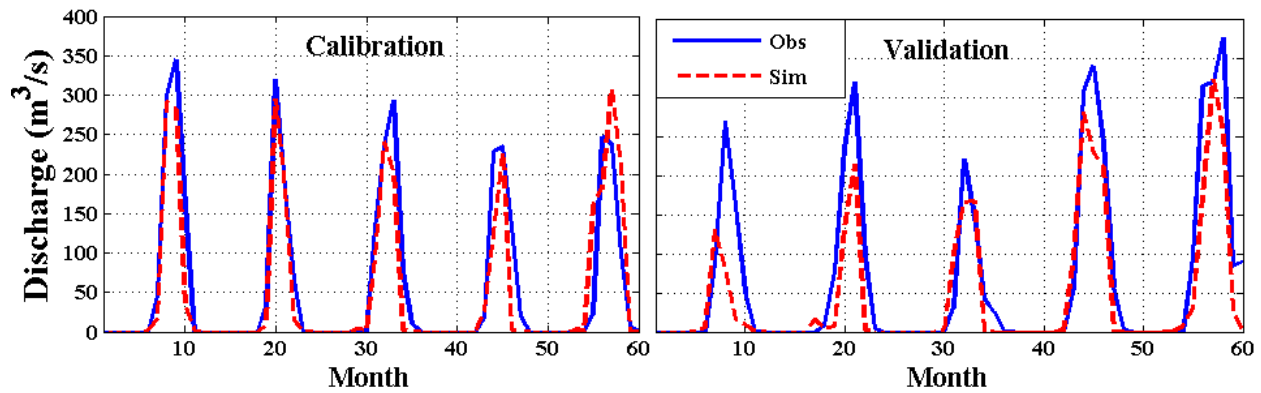
Figure 4. SWAT simulated and observed monthly stream flow in Al Gwisi gauge during the calibration period (1989-1993) (lift panel) and validation period (1995-1999) (right panel), Obs indicates the observed flow and Sim indicates the simulated flow.
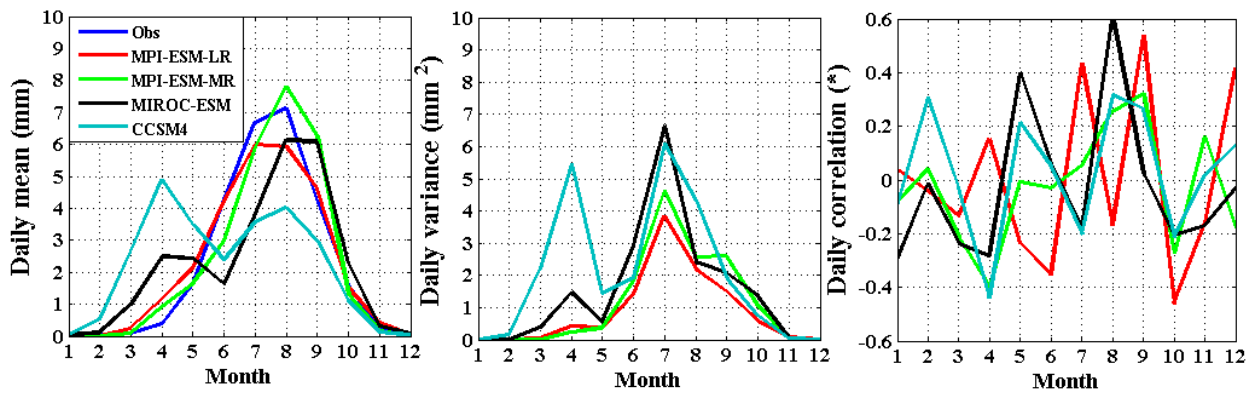
Figure. 5. Comparison between the statistical properties of the observed daily precipitation data for the period 1961– 1990 and the four GCM outputs.

36
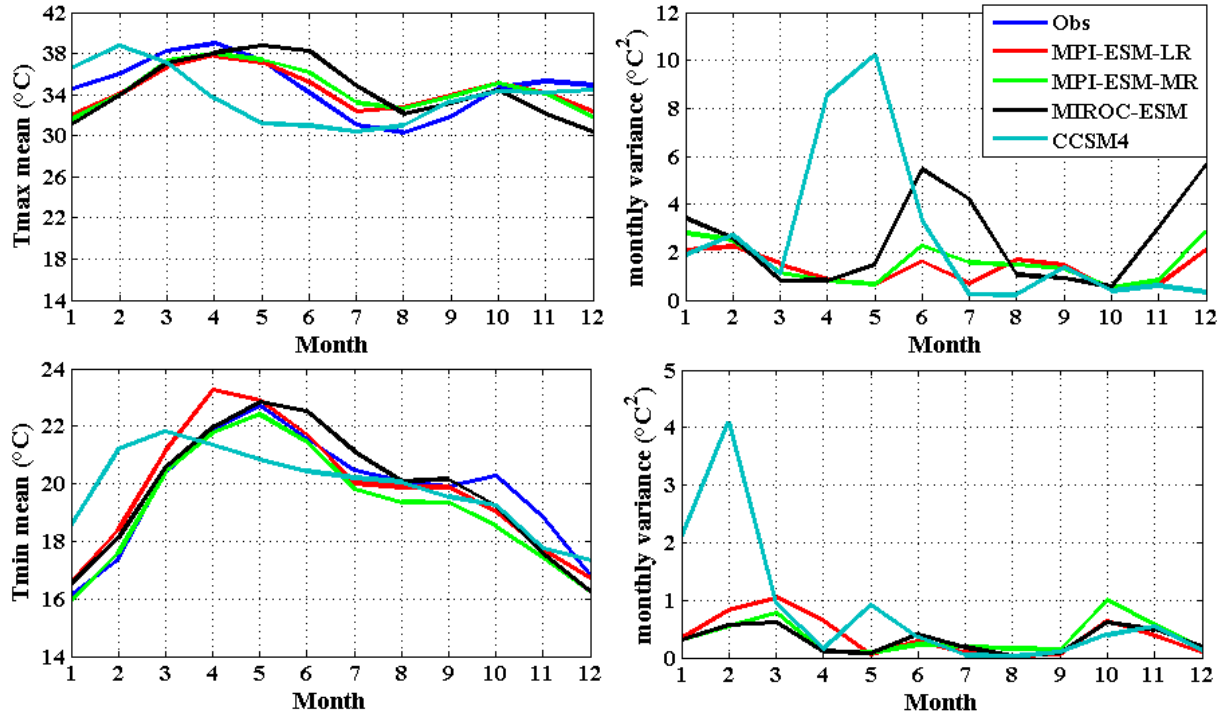
Figure. 6. Comparison between the statistical properties of the observed temperature (1961-1990) and the four GCM outputs; the T_{max} (upper panel) and T_{min} (lower panel) data.
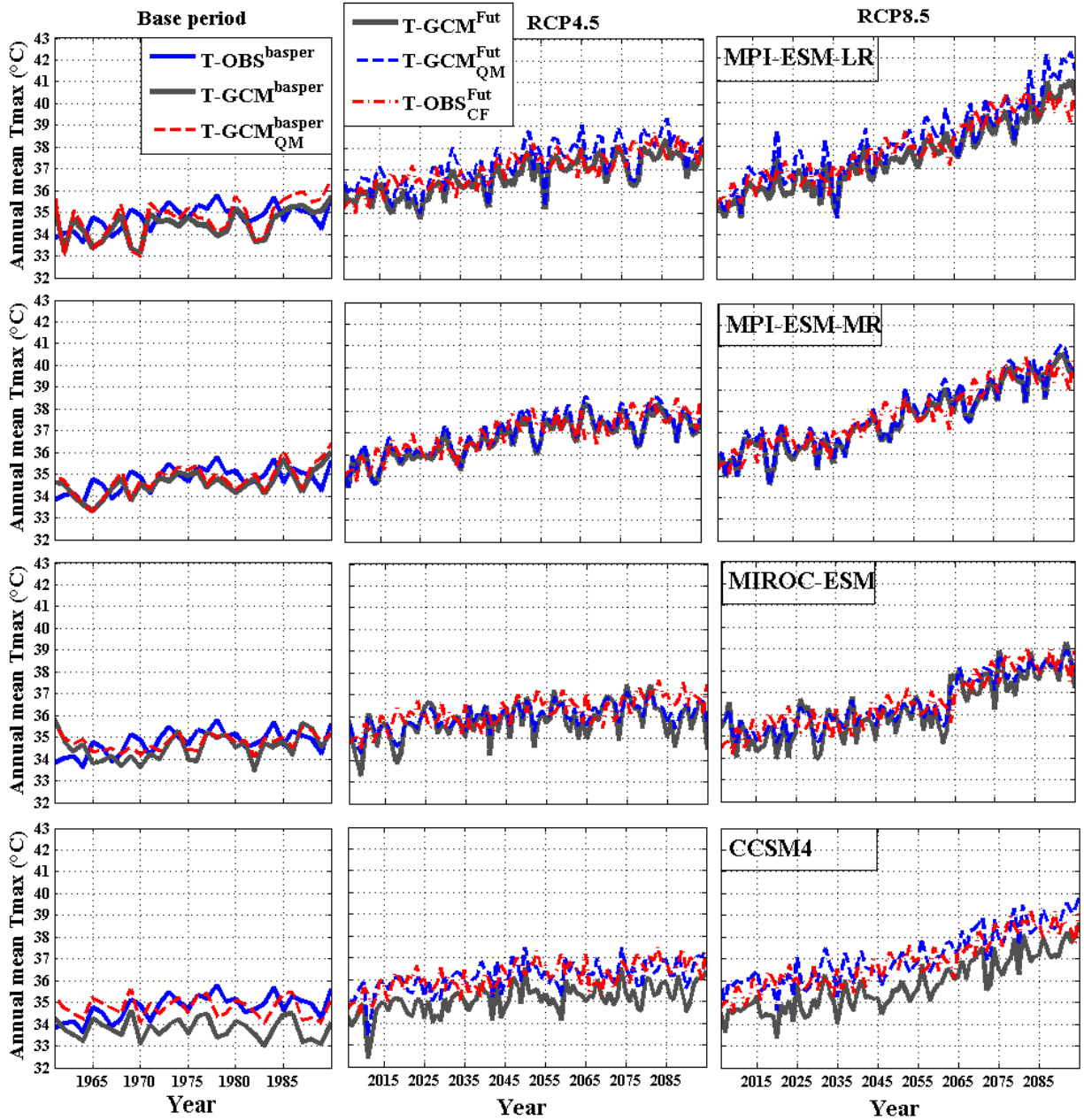
Figure 7. Comparison between the annual T_{max} data observed for the DRB and the results provided by the four GCM models, before (grey line) and after (dashed line) applying the QM approach (CF method is added for the future climate): the Based period; and future climate (for RCP4.5 and RCP 8.5).
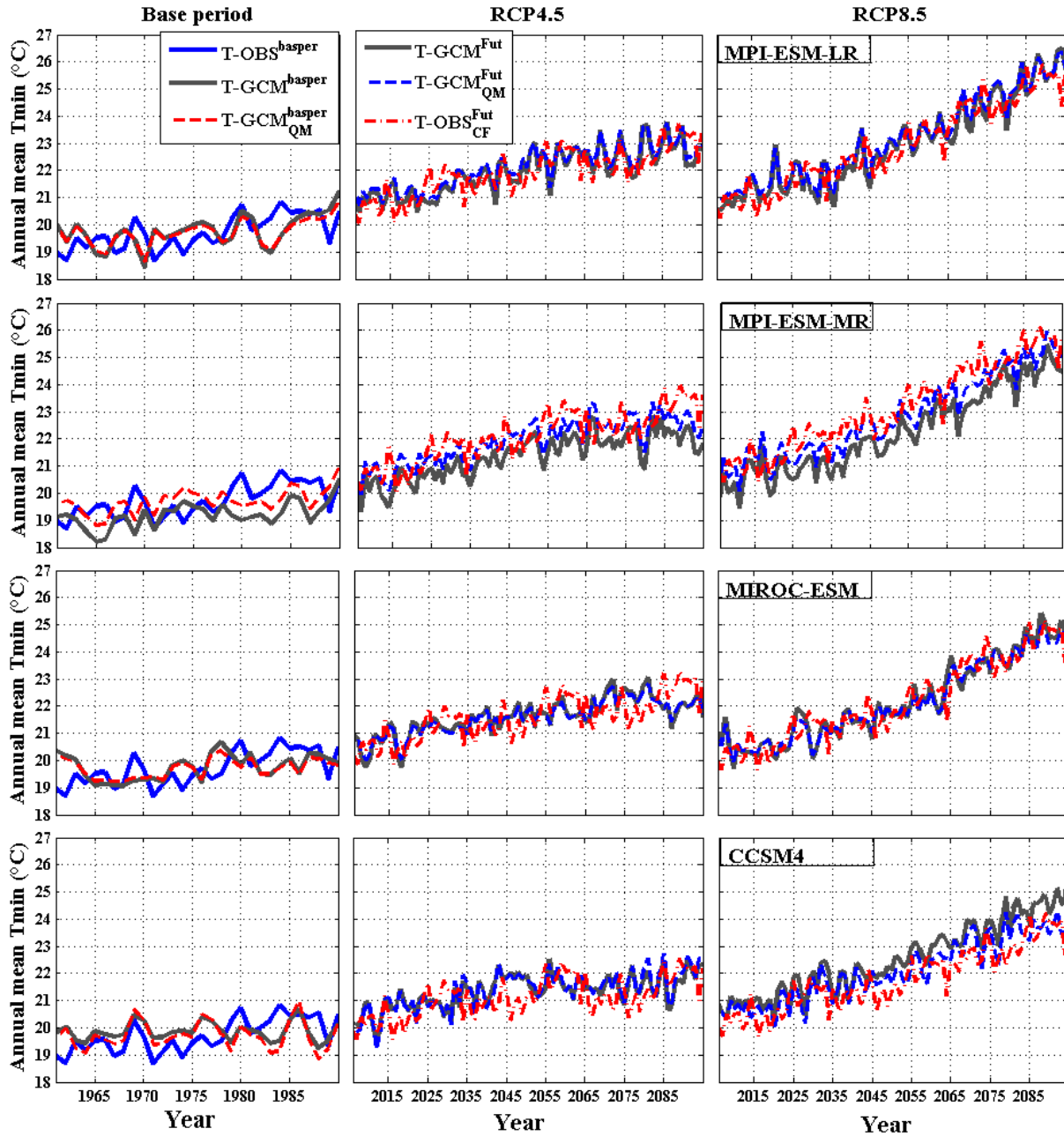
Figure 8. As in Fig. 7, but for the T_{min}.
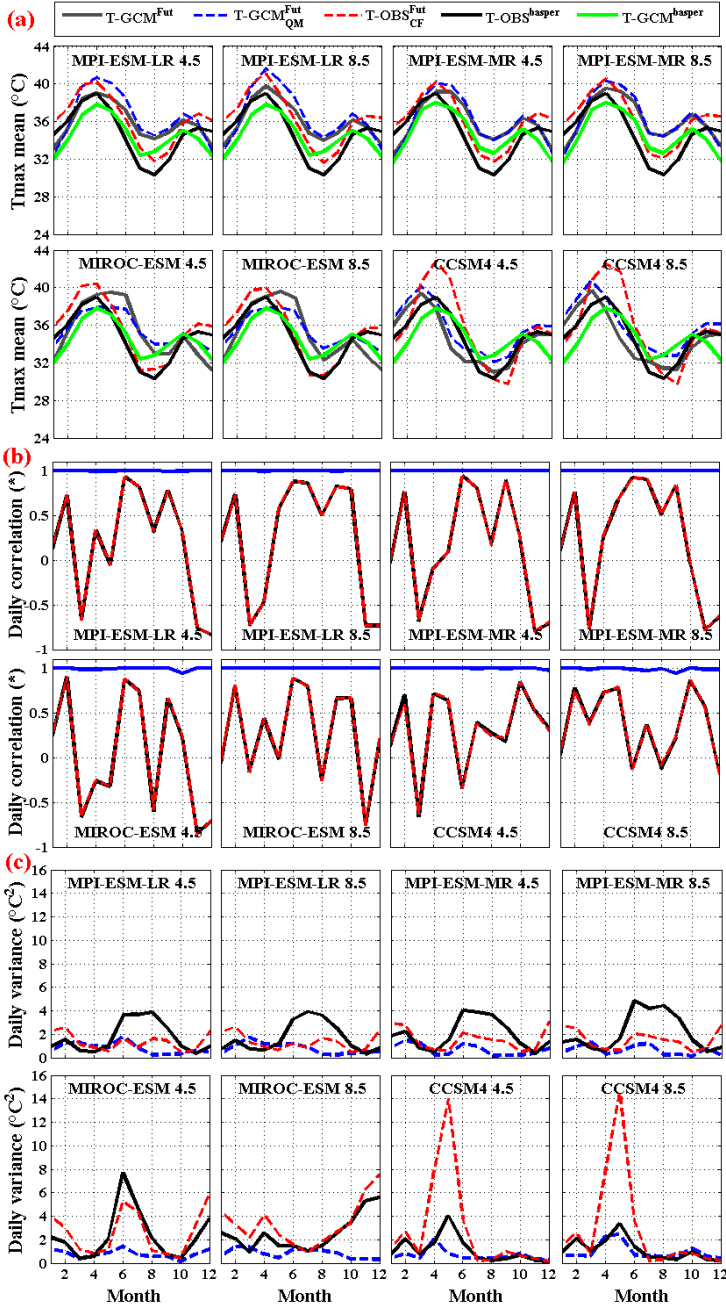
Figure 9. The MPI-ESM-LR, MPI-ESM-MR, MIROC-ESM and CCSM4 models results over the DRB. Comparison at monthly level between the statistical properties of the GCM outputs (T_{max}) data and its downscaled data using the CF ($P - OBS_{CF}^{fut}$) and QM ($P - GCM_{QM}^{fut}$) approaches. For more explanation, the observed data for the baseline period ($P - OBS^{basper}$) are also shown.
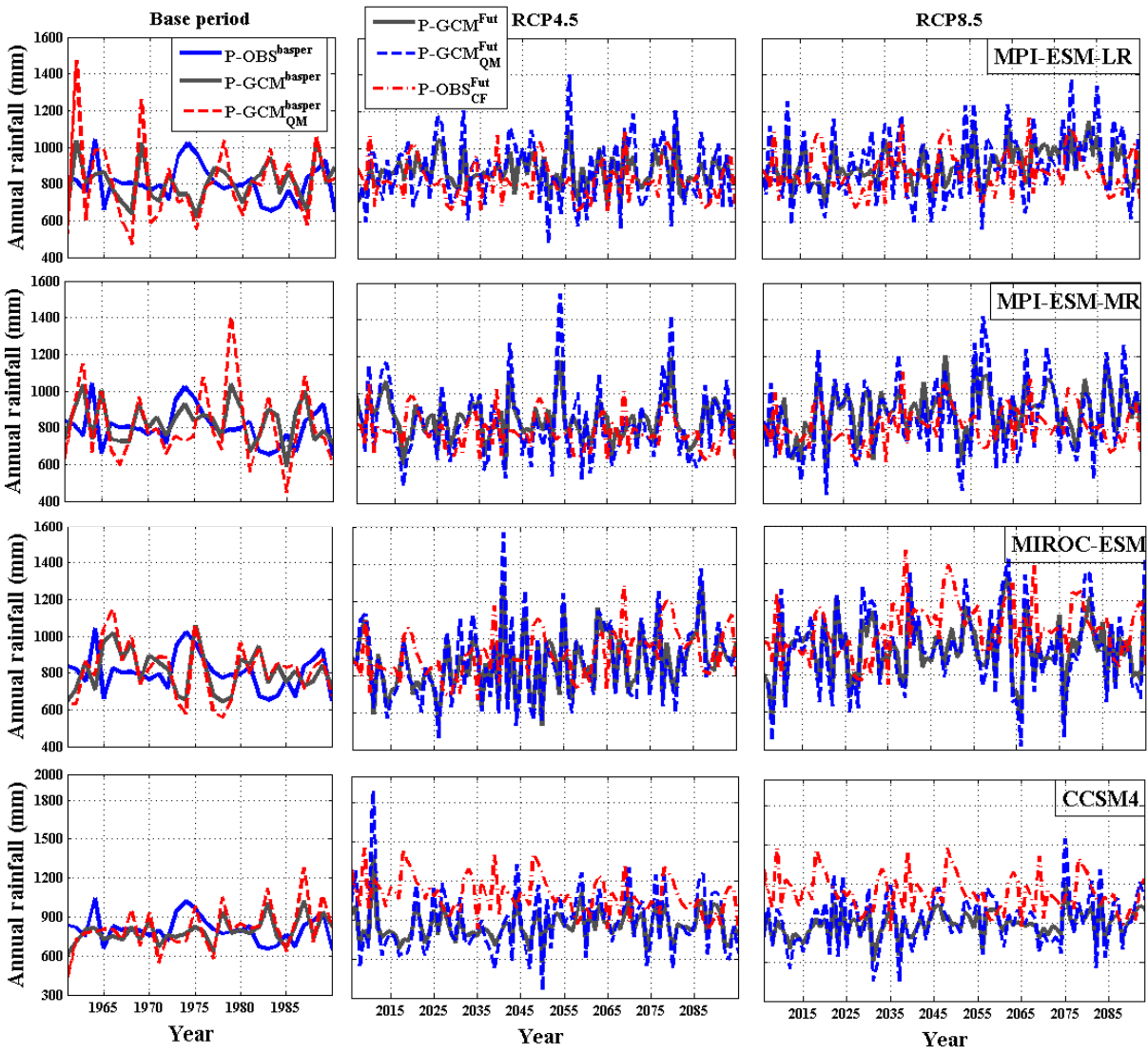
Figure 10. As in Fig. 7, but for the rainfall.
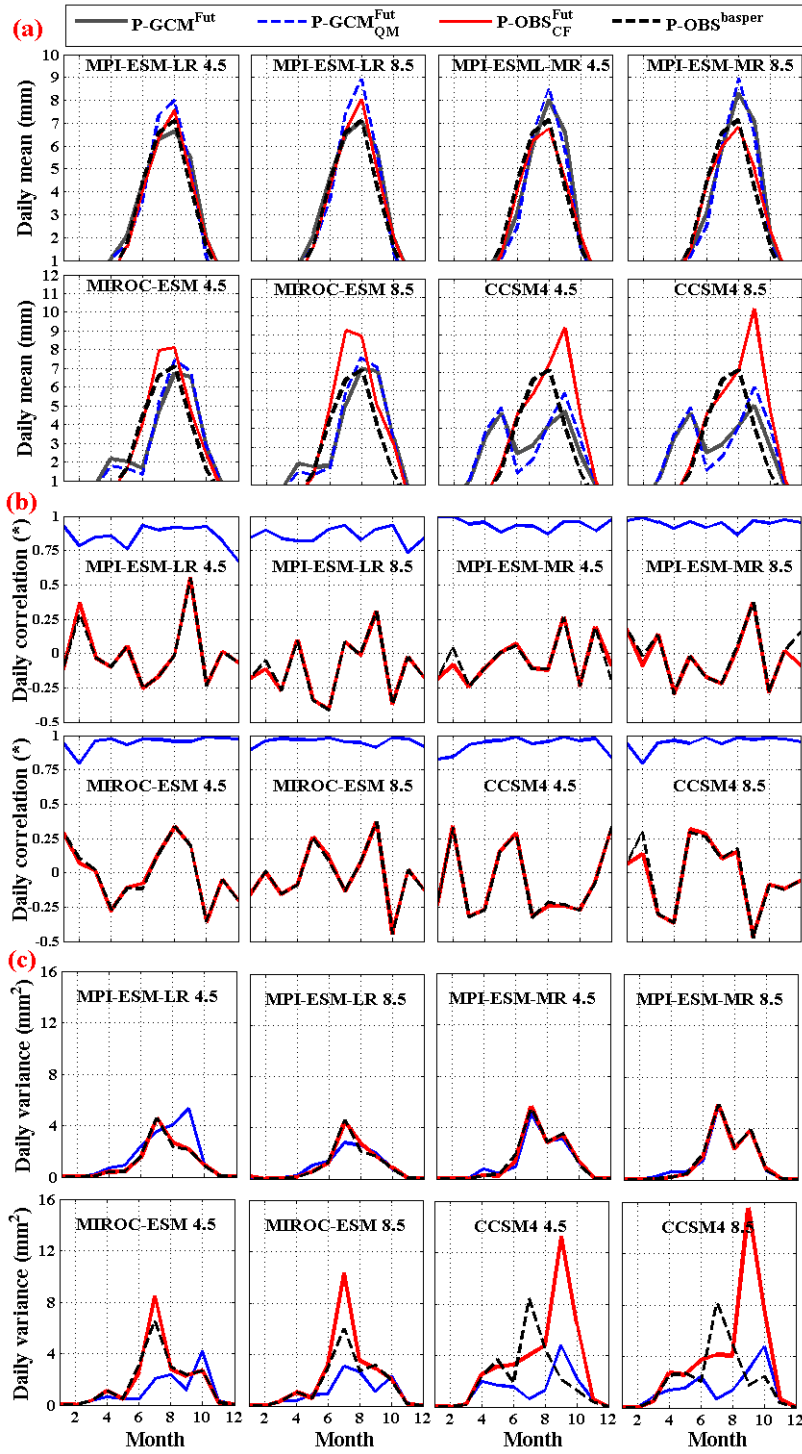
Figure 11. As in Fig. 9, but for the rainfall
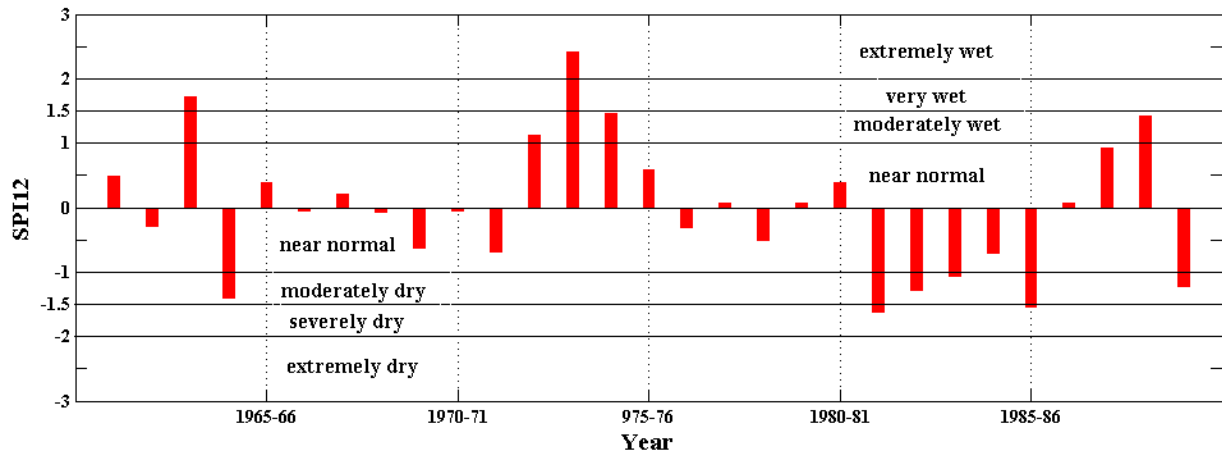
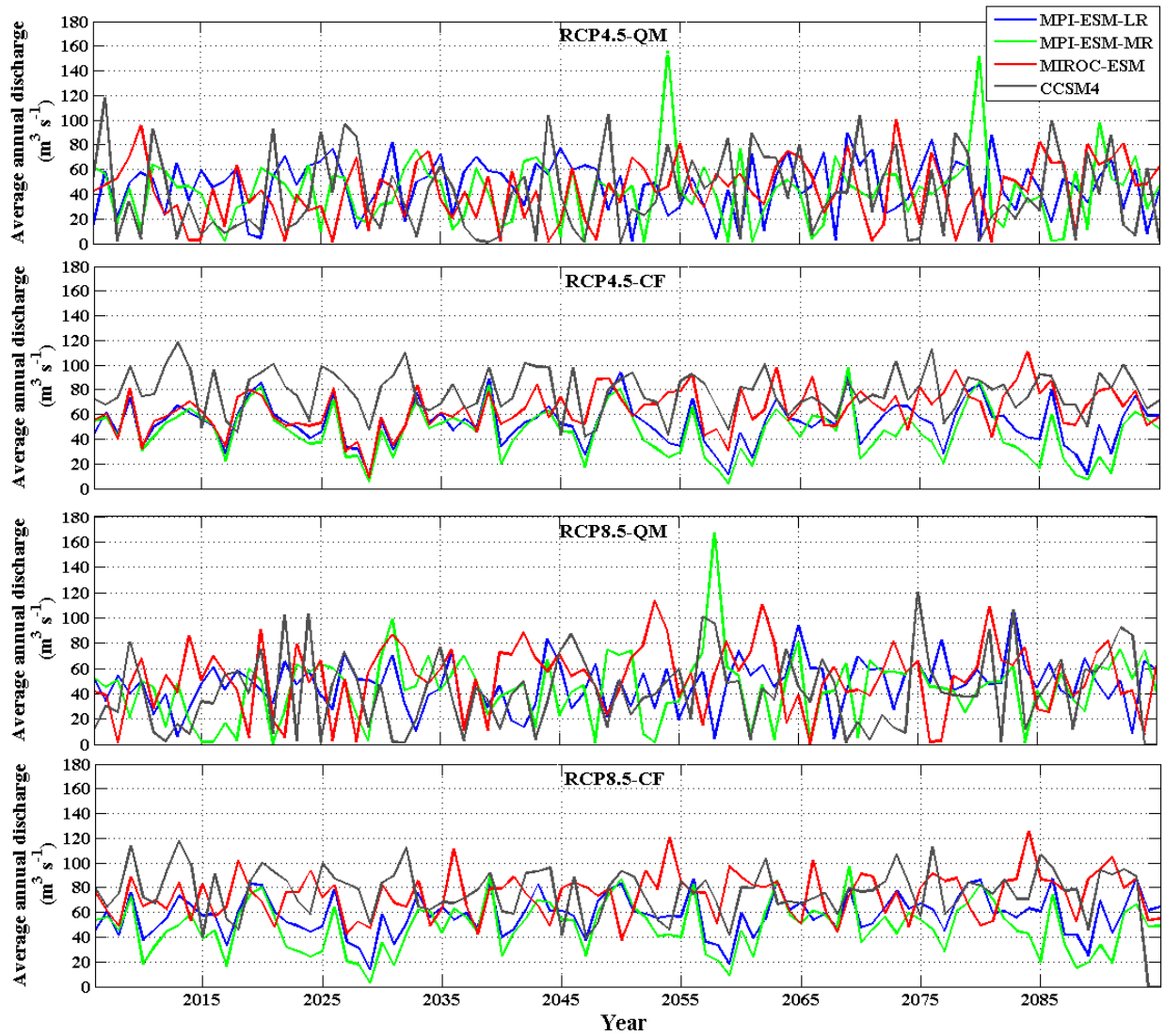Figure 12. Historical time series of SPI for long-term scale

Figure 13. Possible changes in the average annual discharge cycle (on a monthly basis) at the upstream portion of the DRB for the four models when the two downscaling (QM and CF) methods were applied.
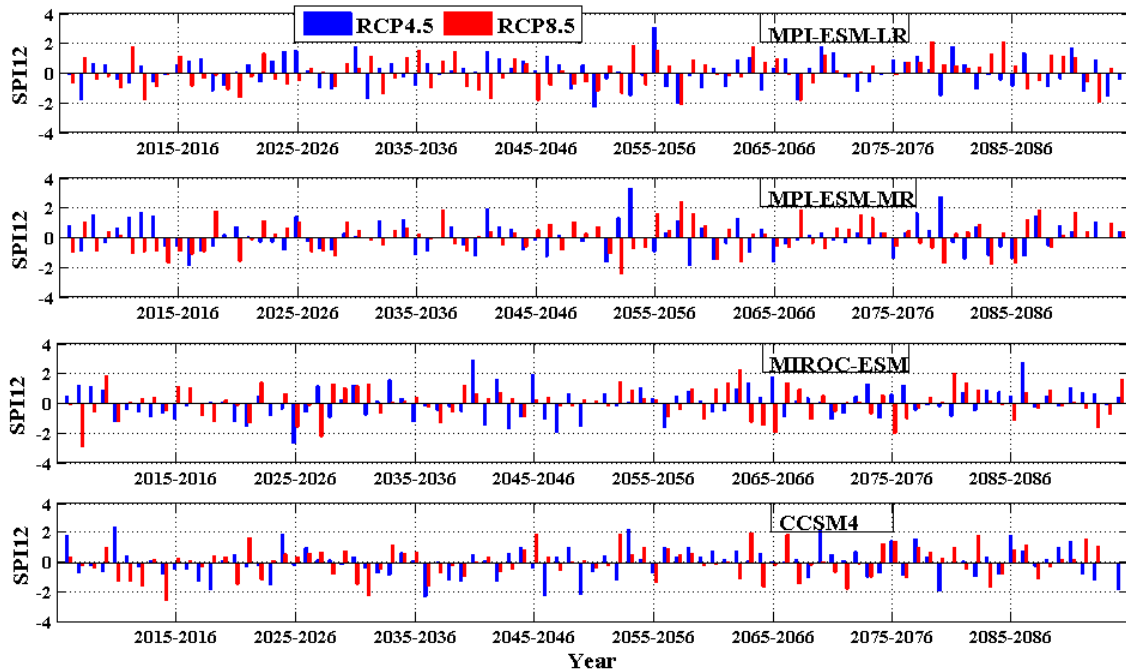
Figure 14. Future time series of SPI-12 (long-term scale) for rainfall projected by the four models and two scenarios (RCP4.5 and RCP8.5) when the QM approach is applied.
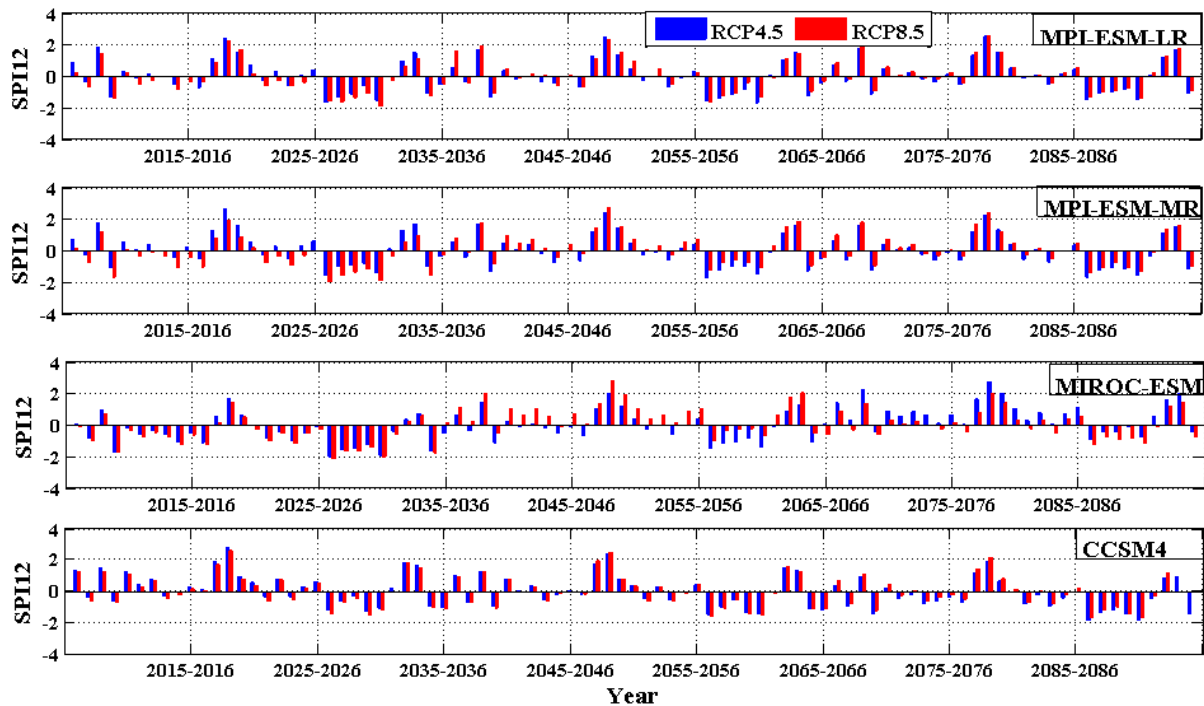

Figure 15. As in Fig. 14, but when the CF approach is applied.